Zeitschrift: Mémoires de la Société Neuchâteloise des Sciences Naturelles
Herausgeber: Société Neuchâteloise des Sciences Naturelles
Band: 12 (1997)

Artikel: Geology of the central Jura and the molasse basin : new insight into an evaporite-based foreland fold and thrust belt = Géologie du Jura central et du bassin molassique : nouveaux aspects d'une chaîne d'avant-pays plissée et décollée sur des couches d'évaporites
Autor: Sommaruga, Anna
Kapitel: 3: Structures : overview, examples and interpretation
DOI: https://doi.org/10.5169/seals-100855

3. STRUCTURES:
OVERVIEW, EXAMPLES AND INTERPRETATION

3.1. INTRODUCTION

The Jura arc on a large scale shows all characteristic features of a foreland fold and thrust belt developed above a weak basal décollement (DAVIS & ENGELDER, 1985; RODGERS, 1990; LAUBSCHER, 1992; TWISS & MOORES, 1992). These features include the arcuate outward convex shape, folds, thrusts and tear faults, that are all kinematically compatible with a tectonic transport in a general NW direction.

Seismic lines have allowed lateral correlation of the well known surface structures from the Haute Chaîne Jura to the less well known adjacent areas of the Molasse Basin hinterland and the Plateau Jura foreland (Fig. 1.2). Different types of folding styles have thus been identified: the Molasse Basin and the external Plateau Jura present broad, long wavelength, low amplitude folds cored by Triassic evaporites; by contrast, the Haute Chaîne Jura is characterized by high amplitude folds which formed above thrust faults stepping up from the basal Triassic décollement. Despite the fact that seismic lines across such folds are of mediocre quality as compared to Melville Island (HARRISON, 1995), they provide important geometric constraints which are most helpful in the construction of viable kinematics model.

The characteristics and particularities of the Jura fold thrust belt and its connection with the Molasse Basin are the result of a series of boundary conditions (see also Chapter 1); the most important are summarized below :

1) presence and thickness variations of a suitable basal décollement zone laid down in form of evaporites and shales during the Triassic (compare Fig. 2.5)

2) the rheological stratigraphy of the Mesozoic carbonate cover with alternating competent limestones and incompetent marl series (Fig. 2.30)

3) the overall wedge shape of the Mesozoic and Cenozoic cover in the Alpine foreland - a result mainly of the Oligocene collision which produced a pronounced foreland basin filled with the clastic Tertiary Molasse wedge.

In this Chapter, a brief theoretical introduction to folds will be given prior to presentation of the actual structures observed. The seismic expression of compressional structures developed in the Jura fold and thrust belt and in the Molasse Basin during the Miocene are discussed. The most prominent structures are high amplitude, thrust-related folds of the Haute Chaîne Jura as well as low amplitude, broad buckle folds developed in the Plateau Jura and the Molasse Basin. Folds and thrusts are intimately linked with the concomitant formation of tear faults. Seismic examples of these structures are compared with field observations on various scales. The lateral continuity of the structures described below will be discussed further in a regional context in the next Chapter 4.

3.2. FOLDS AND THRUSTS

3.2.1. Geometry and mechanisms: definitions

Apart from thrust faults, folds are the most prominent structures developed in the compressional tectonic regime. Folds are ubiquitous from the grain scale (e.g. kinked mica flakes) to kilometers (folded sedimentary series), to the scale of some hundred kilometers (lithosphere flexure). Reflecting this wide range, there is an overwhelming amount of literature which discusses the geometry, kinematics and mechanisms of folds and folding e.g. RAMSAY (1967), SUPPE (1985), TWISS & MOORES (1992), JOHNSON & FLETCHER (1994) and many others. Despite the apparent similarities of folds developed at various scales and in widely different materials, there seems to be no common classification between folds developed plastically, without failure (e.g. in high temperature deformed terranes) and folds developed brittly and often related to faults (e.g. low temperature terranes). Therefore, before describing the Jura and Molasse Basin folds, a summary of definitions and concepts related with folds and folding is given.

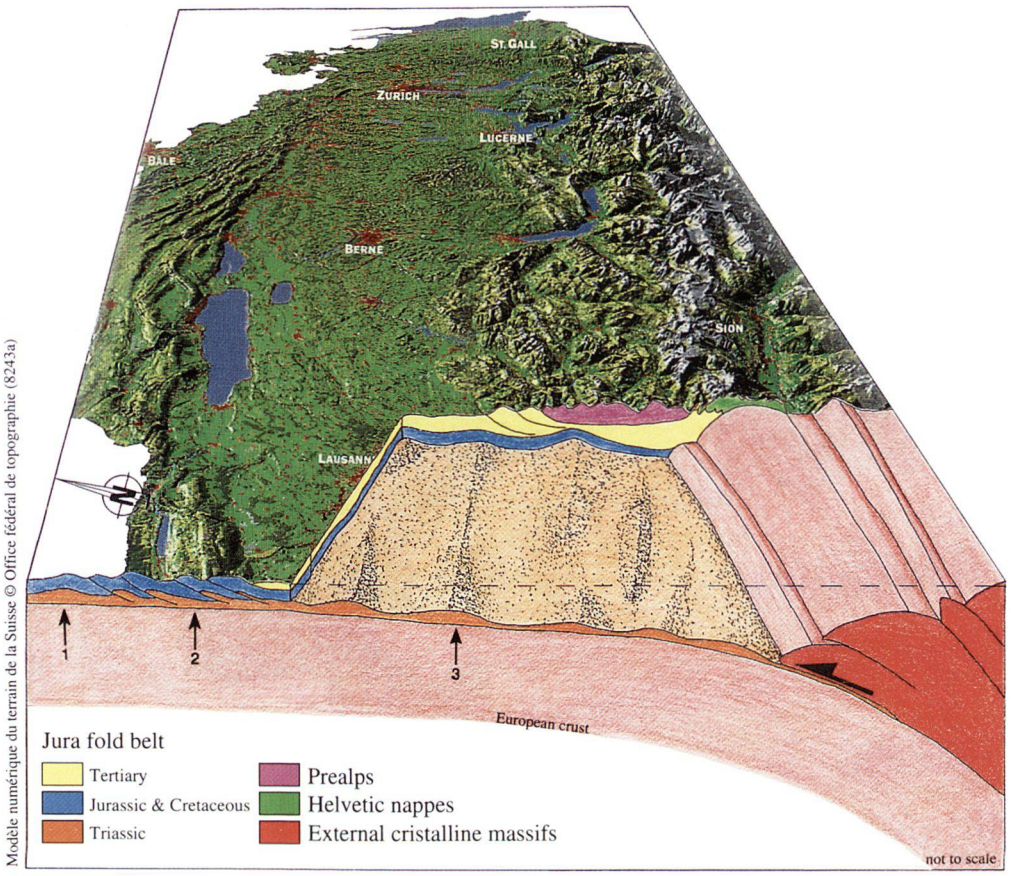

Figure 3.1: Schematic cross-section and bloc-diagram crossing the Jura fold and thrust belt from the foreland to the hinterland. The 3 styles of folds are represented: 1) evaporite-related anticline from the Plateau Jura, 2) thrust- related anticline from the Haute Chaîne Jura, 3) evaporites-related pillow from the Molasse Basin. From SOMMARUGA (1995).

Bloc diagramme schématique recoupant la chaîne plissée du Jura depuis l'avant-pays aux parties internes. Trois styles de plis sont représentés: 1) dans les Plateaux jurassiens, un anticlinal associé à un empilement d'évaporites, 2) dans la Haute Chaîne jurassienne, un anticlinal associé à une rampe de chevauchement, 3) dans le Bassin molassique, un coussin d'évaporites. Tiré de SOMMARUGA (1995).

3.2.1.1. Geometric classifications of folds

Different geometric classifications of folds have been proposed. The most popular fold classification scheme was introduced by RAMSAY (1967) and is based on the comparison of the two surfaces of one layer using any of the following parameters : orthogonal thickness, thickness parallel to the axial plane and the angle of dip isogons with respect to the axial plane. An alternative method by TWISS & MOORES (1992, p.229) describes the style of a fold using its aspect ratio (ratio between the amplitude of a fold and the distance measured between the adjacent inflection points), tightness (interlimb angle) and bluntness (curvature of the fold). The latter and other purely mathematical descriptions (Fourier transform series) have not gained much attention among structural geologists. Although these classifications are purely descriptive and not genetic, they are clearly designed for the description of continuous smoothly folded layers i.e. buckle folds and do not include in their description any discontinuities such as associated thrust faults.

Fault-related folds on the other hand are classified in a totally different, genetic classification scheme. Three end members of fault-related folds, which result in distinct fold-thrust (ramp) interactions, are generally agreed (JAMISON, 1987; MITRA, 1992) (Fig. 3.2):

- fault-bend folds (Fig. 3.2a): folds generated in the hangingwall rocks by movement of a thrust sheet over a ramp (RICH, 1934; SUPPE, 1983). The décollement ramps from a lower structural level over a higher stratigraphic level. The fold develops as a result of the underlying flat-ramp geometry. Fault

bend folds were described first by Rich, in the Pine Mountain thrust region of the Appalachians. He recognized that this fold style developed broad flat-topped symmetric anticlines.

- fault-propagation folds (Fig. 3.2b): asymmetric folds, with one steep or overturned frontal limb associated with a thrust fault. These are generated at the tip of contemporaneously developing thrusts, which propagate into undeformed strata (SUPPE, 1985). As long as the structure has not been faulted through (breakthrough), fault slip is consumed by folding of the overlying strata.
- detachment folds (Fig. 3.2c, d): symmetric or asymmetric folds developed above the termination of a detachment or a bedding parallel thrust fault. The folding does not require a ramp and thus the detachment folds are not associated with ramp thrusts (JAMISON, 1987; MITRA, 1992). Lift-off folds, chevron type (Fig. 3.2e) or box type folds (Fig. 3.2f) are a particular expression of fault-propagation folds and detachment folds. The beds and the detachment are isoclinally folded in the core of the anticline (MITRA & NAMSON, 1989).

The important parameters used for the geometric description of these fault-related folds are the angular relationships between the forelimb, the ramp and the backlimb dip. The emphasis in this classification scheme lies on the description of the geometry of the thrust fault and the overall shape of the fold above.

The consideration of a temporal relationship between folding and faulting is implicit in the description of these folds. Whereas the fault-bend folds develop subsequent to ramp formation, fault-propagation folds and detachment folds develop simultaneously with the ramp or the décollement propagation, respectively. Detachment folds like fault-propagation folds develop at the termination of a thrust fault.

In addition to the three basic end member fault-related fold types, a virtually endless and somewhat confusing terminology has been introduced for the geometric description of networks of thrust faults. The reader is referred to BOYER & ELLIOT (1982) and the glossary by MCCLAY (1992).

3.2.1.2. Mechanisms and kinematics of folding

Folds are the result of compression in a layered material where compression is applied in a direction subparallel to the anisotropy i.e. along the length of the layers. Two fundamentally different mechanisms lead thereby to the formation of folds :

1) Buckling
2) Fault-related folding

Buckling and buckle folds

Buckling results from the application of compressive stresses in layered materials with contrasting viscosities (rheologies), where both the strong and the weak materials are plastically deformed without failure. Above a certain threshold of compressive stress, the stiffest layers become unstable and buckle into a fold. Buckling is the dominant folding mechanism at relatively higher temperatures and confining pressures, where deformation is essentially plastic (flowing) and pervasive, although strongly partitioned into the weaker layers. Buckling is the most discussed mechanism in the literature and was first proposed by HALL (1815) and later treated in many text books e.g. BIOT (1957), RAMBERG (1964), RAMSAY (1967), JOHNSON & FLETCHER (1994).

Buckle folds (Fig. 3.2g) may be developed in a single layer or in a multilayer stack. Folding of a single layer means that the layer is embedded in viscous media. The layer has two interfaces and if the two interfaces deflect in the same direction the resulting structure is called a buckle fold. The development of buckle folds in single-or multi-layers has been studied by mathematical and analog models (JOHNSON & FLETCHER, 1994). The most important parameters which control the development of buckle folds are: the viscosity contrast of the materials, the layer thicknesses, as well as the cohesion between layers. The main results can be summarized as follows:

- competent (stiff) layers are less deformed internally than the incompetent matrix
- in stiff layers, deformation is concentrated in fold hinges
- limbs of stiff layers show little internal deformation
- hinges are formed early and remain fixed in the material
- wavelength is determined by the viscosity contrast and the thickness of the stiff layer

in a multilayer:

- strong layers influence each other

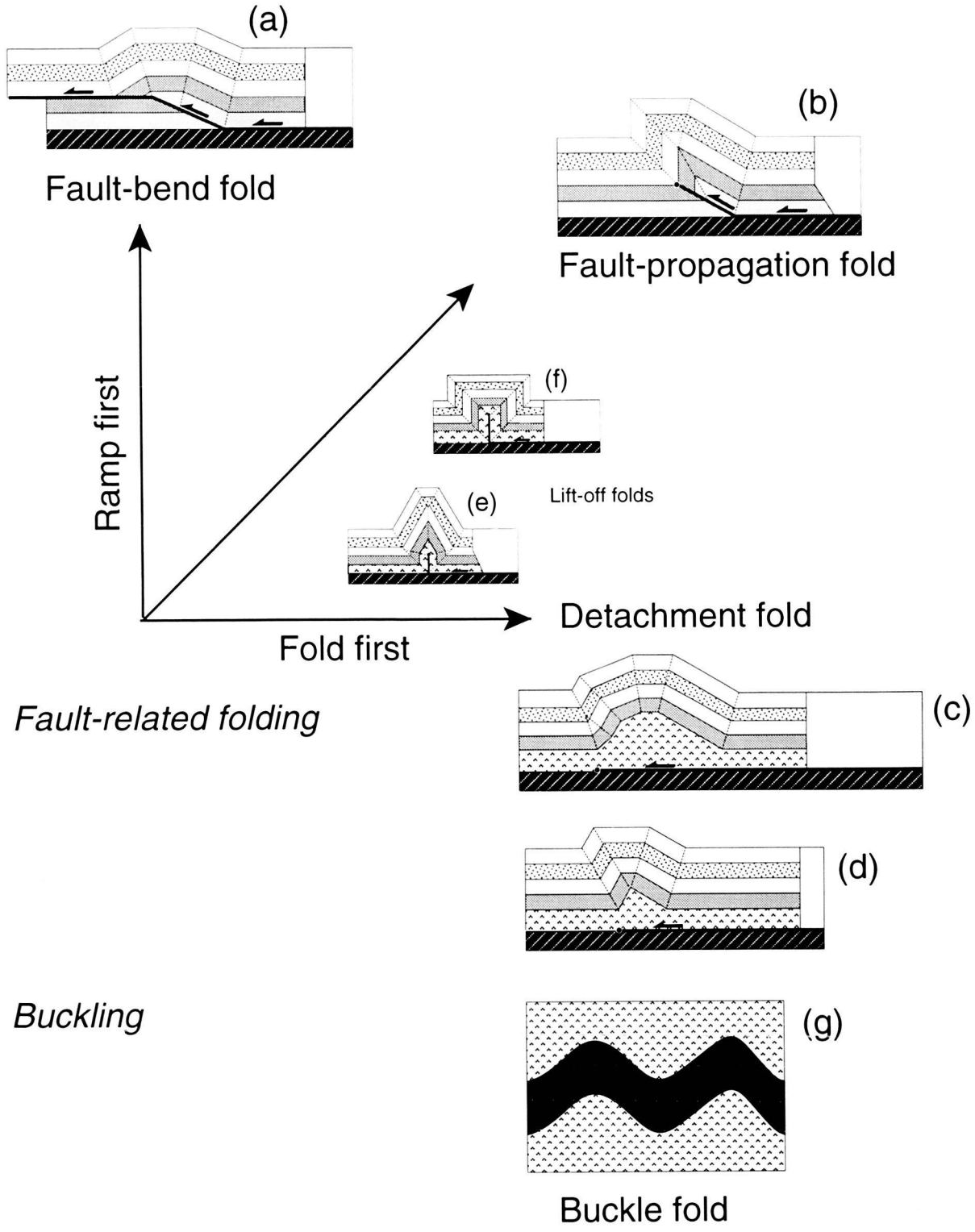

Figure 3.2: Geometry of folds (see text for discussion). Classification of fault-related folds: a) fault-bend fold (RICH, 1934; SUPPE, 1983); b) fault-propagation fold (SUPPE, 1985; SUPPE & MEDWEDEFF, 1990; MOSAR & SUPPE, 1992); c) detachment fold from MITRA (1992); d) detachment fold from JAMISON (1987); e) chevron type of lift-off fold (MITRA & NAMSON, 1989); f) box fold type of lift-off fold. Classification of buckle fold: g) buckle fold with a single layer.

Géométrie des plis (voir texte pour discussion). Classification des plis associés à une faille: a) fault- bend fold (RICH, 1934; SUPPE, 1983); b) fault-propagation fold (SUPPE, 1985; SUPPE & MEDWEDEFF, 1990; MOSAR & SUPPE, 1992); c) detachment fold de MITRA (1992); d) detachment fold de JAMISON (1987); e) type chevron du lift-off fold (MITRA & NAMSON, 1989); f) type coffré du lift-off fold. Classification des plis de flambage: g) pli de flamblage à une seule couche.

- the most resistant (viscosity and thickness) layer dictates the dominant wavelength

Multilayer sequences contain layers of widely different strength and thickness. According to experiments, the form of the folds depends upon several parameters: the relative stiffness of the multilayer and its confinement; the relative thickness and stiffness of adjacent layers within a multilayer; the properties of the contacts between layers; the degree of cohesion between layers. Experimental measurements (JOHNSON & BERGER, 1989) in sedimentary rocks shows that if there are too few ductile layers in a multilayer stack, the stack will fail by faulting before it buckles into folds.

Fault-related folding and fault-related folds

The second mechanism of fault-related folding requires a fault to be active prior to and/or during fold formation. This mechanism does not require any viscosity contrast, nor does anisotropy have to be present in the material other than that of a localized thrust fault. This mechanism develops in the low temperature regime, where deformation is predominantly brittle.

Folds related to a ramp active prior to folding (Fault-bend folds) were first described by RICH (1934). He proposed that the thrust surface followed some zone of easy gliding, such as shale until frictional resistance became too great and then sheared diagonally up across bedding forming a ramp to another shale, then following the shale for some distance, to shear across the bedding at another ramp to the ground surface. This mechanism (ramp folding) was later discussed more precisely by WILTSCHKO (1979) and by JOHNSON & BERGER (1989). A ramp fold is the result of duplication of strata at the ramp fault and along the detachment surface beyond the ramp fault. Folds are consequently formed passively by translation of a thrust sheet over a ramp. In this model, the thrust is clearly implied to develop first and the fold is a product of passive accommodation. The model has the advantage of being easy to analyze in a rigorous geometrical way. A problem with this model is the location of the ramp.

Another model is represented by folds which develop simultaneously with the ramp portion of a stepped thrust fault (fault-propagation folds). The mechanisms of those folds are not so well understood as yet.

Fault-related folds are developed in a multilayer sequence assuming bedding plane slip between the layers. Fault-bend and fault-propagation folds are formed over a discrete sole thrust and represent a folded multilayer sequence with a very low viscosity contrast between layers. Detachment folds require a weak décollement layer (e.g. salt or shale layer), which can infill the space generated at the base of the fold. The latter have all the characteristics of a buckle folds.

The nucleation of the faults is an interesting question. Models proposed by DIXON & LIU (1992) based on centrifuge modeling, suggests that, in a stratigraphic sequence with high contrast of viscosity between layers, the thrust ramps are localized solely by earlier stage of low amplitude folds. Early buckling would be responsible for the localization of the ramps.

Criteria to distinguish buckle and fault related folds ?

The most obvious criterion for the distinction of the two folding mechanisms is the identification of a thrust fault which can genetically be related to the fold formation. In the case of folds observed in foreland fold and thrust belts, this usually requires a detailed knowledge of the subsurface geometry, which may often not be available.

The fold profile may provide some information about the relative competency of layers. However, there is no information regarding the underlying dominant folding mechanism (buckling vs. fault-related folding).

A detailed knowledge of the internal deformation along the entire fold profile, in individual key layers, may provide other critical information about the folding mechanism: deformation can be expected to be concentrated within fold hinges of competent layers of buckle folds, whereas intricate but predictable patterns of high and low strain zones (possibly several superposed incremental strain "events") may be expected throughout in fault-related fold models, where material has to move through certain axial planes.

Transitions between buckle folds and fault-related folds

Transitions from buckling to fault-related folding mechanisms are commonplace and accordingly, there is no clear cut limit between the two end mem-

ber mechanisms of folding. Folding may start by buckling of a competent layer to a certain amount of shortening, before deformation is localized into thrust faults (DIXON & LIU, 1992). Alternatively, a sedimentary wedge may start to deforme by thrust faulting and then be buckled at later stages. Moreover transitions between the two models of fault-related folding (fault-propagation folds to fault-bend folds) are also possible.

3.2.1.3. Kinematic sequences associated to salt flow

The presence of weak layer in a multilayer sequence has a strong influence on the mechanisms of folding. Rock salt, one of the weakest material known in sedimentary sequences, is responsible for a particular set of deformation structures.

Salt tectonics (syn. halotectonics) refers to any tectonic deformation involving salt or other evaporites as a substratum or a source layer (JACKSON & TALBOT, 1994). Halokinesis, on the other hand, designates the formation of salt structures which are the result of salt flow under the influence of gravity alone, without any significant lateral tectonic forces (TRUSHEIM, 1957, 1960).

In the studied area, gravity forces are not unique and probably not the most important. A major lateral push of the Alps towards the NW appears to be responsible for the formation of the Jura foreland fold and thrust belt. This stress is well known under the German term "Fernschub" (= distant push) defined by LAUBSCHER (1961).

In sedimentary environments, the continuous deposition of layers during salt movements may record the timing and the character of the salt flow. Three kinematic sequences have been distinguished (Fig. 3.3). The prekinematic sequence is deposited before the salt starts to flow; the synkinematic sequence is deposited during the salt flow and shows internal onlaps or truncations; the postkinematic sequence is deposited after the salt stopped flowing. The recognition of these sequences in a mountain belt, may give many information on the timing of deformation. In the field, evidence may also be furnished by thickness changes and truncations or onlaps. High quality seismic lines may be required to reveal all the subtleties of such salt structures and their relation with the surrounding rocks.

3.2.2. Evaporite-related folds (low amplitude)

3.2.2.1. General comments

Low amplitude folds may be difficult to recognize on geological maps or in the field. The low limb dip and the low structural relief make these structures inconspicuous and difficult to observe at outcrops. Seismic lines are more useful in documenting the geometry of this fold type at depth.

Interpretations of seismic lines across the Plateau Jura and the Molasse Basin, show a series of broad and gentle anticlines which are controlled by evaporite, salt and clay stacks within the ductile Unit 2 of the Triassic layers.

In the scientific literature, this type of anticline is termed salt anticline or salt welt (HARRISON & BALLY, 1988) also defined by JACKSON & TALBOT (1994) as "an elongated upwelling of salt with concordant overburden". The term salt pillow has the same meaning, but is used for subcircular shapes (Fig. 3.4). In this work, we prefer to use the terms evaporite anticline and evaporite pillow, due to the uncertainty about the amount of pure salt in the Triassic layers. Conventional salt pillows, as first visualized by TRUSHEIM (1960), are today often interpreted in an overall extensional context (VENDEVILLE & JACKSON, 1992). In a compressional context, ideally, the evaporites pinch out in the adjacent synclines and flow into anticlinal evaporite ridges (HARRISON, 1995).

It is important not to confuse the term salt welt with the term salt weld, which describes a surface or zone of adjacent strata originally separated by autochthonous or allochthonous salt (JACKSON & TALBOT, 1989). Compressional salt welds occur when all ductile material has migrated from the syncline to the core of the anticline.

3.2.2.2. Geophysical evidence from seismic profiles

Geophysical evidence for evaporite stacks include thickness variations of a seismic unit, which are spatially associated with broad folds in the overlying formations and velocity anomalies. The latter generally consist of a positive deflection of the reflectors (velocity pull-up) beneath anticlines, caused by the thickening of the Triassic evaporite unit of supposedly high velocity. This velocity pull-up is further enhanced by a velocity pull-down in the synclines,

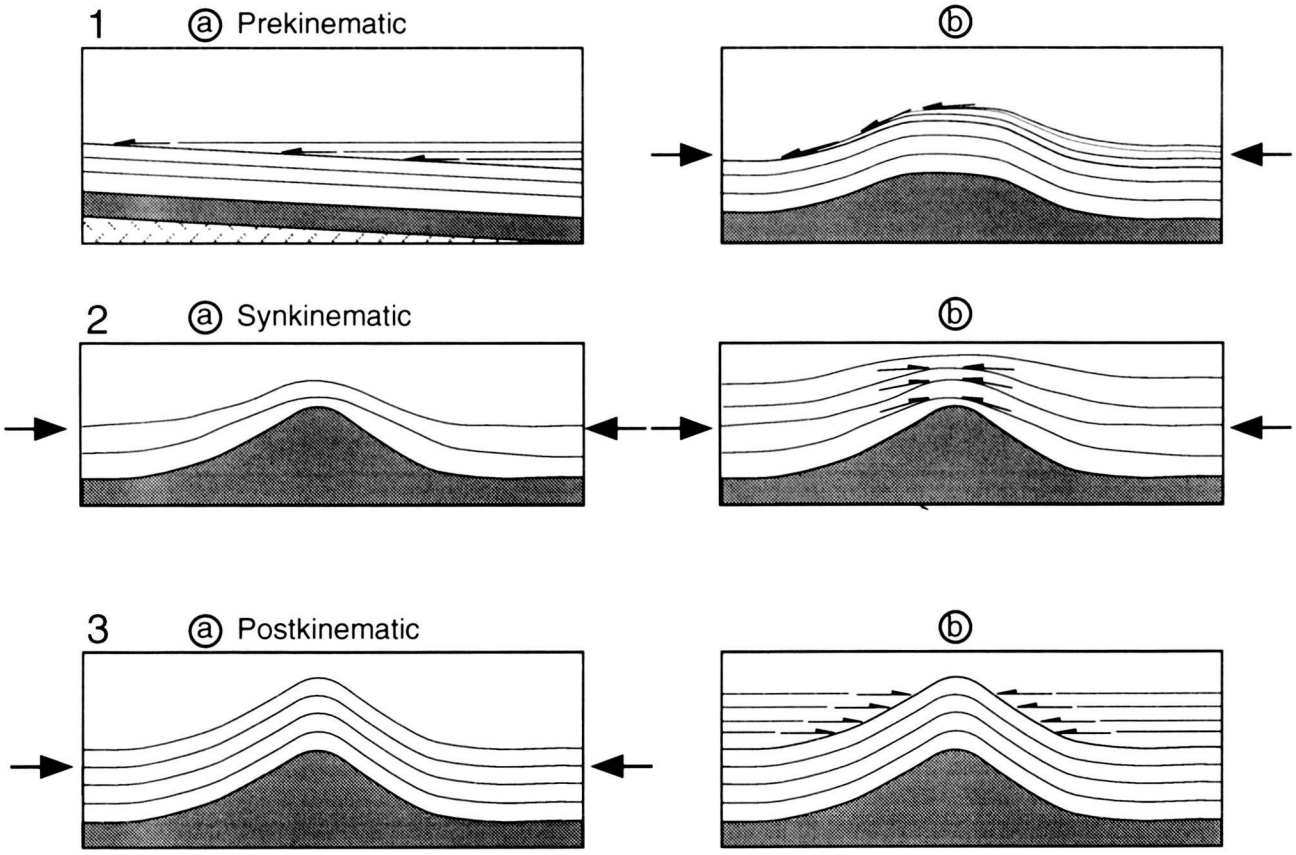

Figure 3.3: Sedimentary record of salt flow during shortening. Three kinematic sequences are inferred from the relation salt flow and sedimentary record. 1) Prekinematic sequence; 2) Synkinematic sequence; 3) Postkinematic sequence. Inspired from JACKSON & TALBOT (1994).

Enregistrement syn-sédimentaire du fluage du sel durant un raccourcissement. Trois séquences cinématiques sont déduites des relations entre le fluage du sel et l'enregistrement sédimentaire. 1) Anté- cinématique; 2) Syn-cinématique; 3) Post-cinématique. Inspiré de JACKSON & TALBOT (1994).

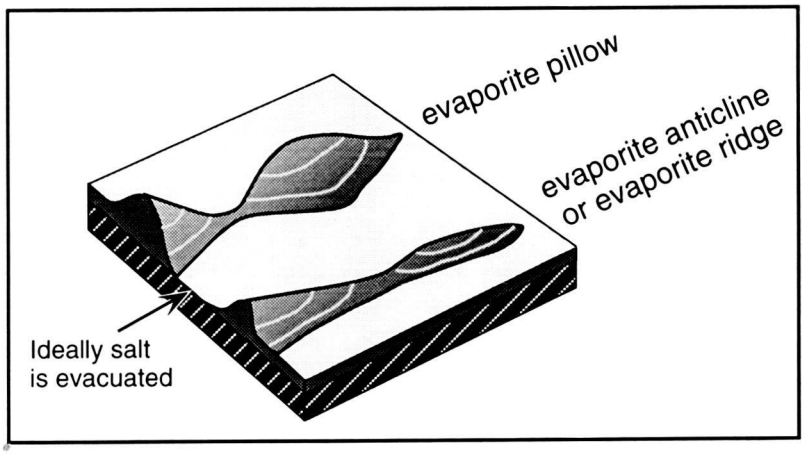

Figure 3.4: Difference between evaporite anticline and evaporite pillow. An evaporite anticline has an elongated shape, whereas the evaporite pillow has a sub-circular shape. Modified from JACKSON & TALBOT (1994).

Différence morphologique entre un anticlinal associé à des évaporites et un coussin associé à des évaporites. Un anticlinal d'évaporites est caractérisé par une forme allongée, tandis qu'un coussin d'évaporites montre une forme sub-circulaire. Schéma inspiré de JACKSON & TALBOT (1994).

due to the low velocity of the thick Tertiary sediments (Fig. 3.8, Essertines anticline). As described in §2.4.3.8. the Triassic Unit 2 shows discontinuous and oblique reflectors, whereas the overlying unit (Triassic Unit 1) displays well layered, laterally continuous reflectors. Triassic Unit 1 does not present thickness changes and seems therefore to be tectonically undisturbed.

3.2.2.3. Examples illustrated by seismic profiles

The Plateau Jura evaporite anticlines

The Plateau Jura broad folds are illustrated on the northern part of the dip Section 111 (Panel 9 and Plate 8) and Sections 107, 115 and 117 (Panel 10). These folds display two long asymmetric limbs dipping with a very low angle towards the North and the South respectively. This geometry is illustrated by a well layered series of reflectors in the middle of the Mesozoic cover series (Fig. 3.5). This sequence represents the evaporites of the Triassic Unit 1. Beneath this unit, we observe discontinuous reflectors belonging to the Triassic Unit 2. Some of these reflectors onlap the last strong and continuous reflection, which represents the top of the basement (either crystalline rocks or Permo-Carboniferous sediments). The Triassic Unit 2, highlighted in dark gray on Figure 3.5, shows a thickness increasing from NW to SE. This thickening, due to evaporite stacking, appears clearly on dip seismic lines (Plate 8, Panel 10 and Fig. 3.5). It is the thickest stack of evaporites observed so far in the studied area and has been confirmed by the Laveron drill hole (BRGM, 1964). The Laveron fold (Fig. 3.5 and Section 107 on Panel 10) is a clear seismic expression of what is here termed evaporite anticline. BITTERLI (1972), over twenty years ago, presented an interpretation referring to halokinetic movements.

Few Plateau Jura anticlines are symmetric. Most, typically exhibit a limb grading progressively into a syncline (thinning of Triassic Unit 2), whereas the opposite limb ends against faults. On Section 107 (Panel 10), the Laveron anticline stops against the Mouthe tear fault trending N-S. On Section 117 (Panel 10), the evaporite anticline disappears towards the South in a transparent zone. The latter corresponds to the transition between the Haute Chaîne Jura and the Plateau Jura, as well as to the intersection between the Morez tear fault, oriented NNW-SSE and the "Faisceau de Syam", a strongly deformed zone oriented NNE-SSW (Figs. 1.2, 4.1 and Panel 10).

It has to be emphasized, that thrust faults (ramp or flat) and repetition within the Mesozoic strata are not recognizable. Sections 111 to 85 (Panel 9) clearly show the geometrical contrast between high amplitude Haute Chaîne Jura folds, related to thrust faults and low amplitude Plateau Jura folds, related to evaporite stacks.

The Molasse Basin pillow structures

In the Molasse Basin, broad anticlines are known from outcrop geology. Interpreted subsurface data (Panel 4, strike lines; Panels 5 and 6, dip lines; Plates 6 and 7) present a succession of low amplitude folds, with slightly dipping limbs. Folds with a high degree of symmetry have been found in the southern region, whereas further to the North they are either foreland- (NW) or hinterland- (SE) verging. The same anticline may also change its vergence laterally (Figs. 3.6, 3.7 and 3.8). The geometry of the folds is highlighted by a well layered series of reflectors representing Cretaceous, Malm, Dogger, Liassic and upper Triassic strata. The core of these folds is filled with thickened Triassic Unit 2 beds and their geometry is shown in detail on the six seismic examples (Figs. 3.7 to 3.12). The location of these parts of seismic lines is shown on Figure 3.6, which represents an isopach map of Unit 2 of the Triassic beds of the western Swiss Molasse Basin. This map highlights elongated or elliptical thickening of the Triassic Unit 2 along a NE-SW trend. The consequential interpretation of these structures and their pattern on formation of the Jura is discussed in Chapter 5.

Triassic Unit 2 is colored in dark gray on the seismic interpretations of Figures 3.7 to 3.12. These examples illustrate the considerable thickness variations and also the internal pattern of the unit. Thickening is located underneath broad anticlines and the maximum thickness coincides with the most internal Jura anticlines (compare Fig. 3.6 and Fig. 3.11). Generally, Unit 2 displays discontinuous reflectors, which are either flat or oblique, bounded by a basal and roof reflector. Examples 2, 5 and 6 (Figs. 3.8, 3.11 and 3.12) show a succession of oblique reflectors within Triassic Unit 2, that dip toward the South. These reflectors may be interpreted as small thrust faults imbricating parts of the unit, to result in an overall thickening. Such structures are named duplexes in the literature (MITRA, 1986; MCCLAY, 1992). Duplexes are bounded by a roof thrust, e.g. below reflector H (Top Triassic Unit 2) and a basal thrust, e.g. above the top of the basement in our study area.

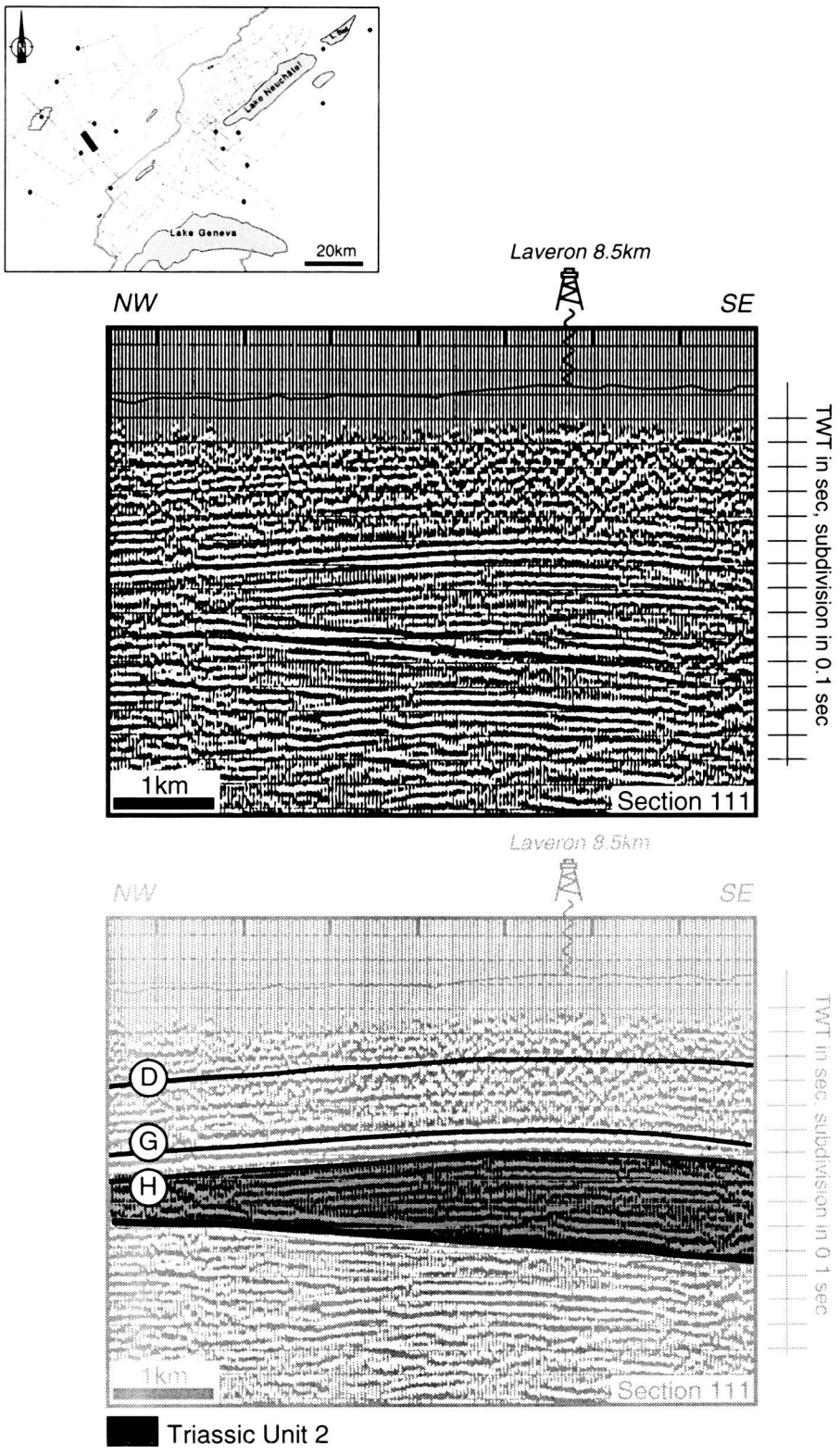

Figure 3.5: Northern part of the dip seismic Section 111 located in the Plateau Jura (external zone). The interpretation displays a broad anticline related to thickening of the Triassic Unit 2. Laveron drill hole (projection), which reaches the top of the Buntsandstein strata, confirms the seismic interpretation. Legend for the top of the layers: D = Dogger; G = Triassic Unit 1, H = Triassic Unit 2.

Partie septentrionale du profil sismique 111 transversal localisé dans les Plateaux jurassiens (zone externe). L'interprétation montre un large anticlinal associé à un épaississement dans l'Unité 2 du Trias. Le forage de Laveron (projeté de 8.5 km) atteint le toit des couches du Buntsandstein et confirme l'interprétation sismique. Légende pour le toit des couches: D = Dogger; G = Unité 1 du Trias, H = Unité 2 du Trias.

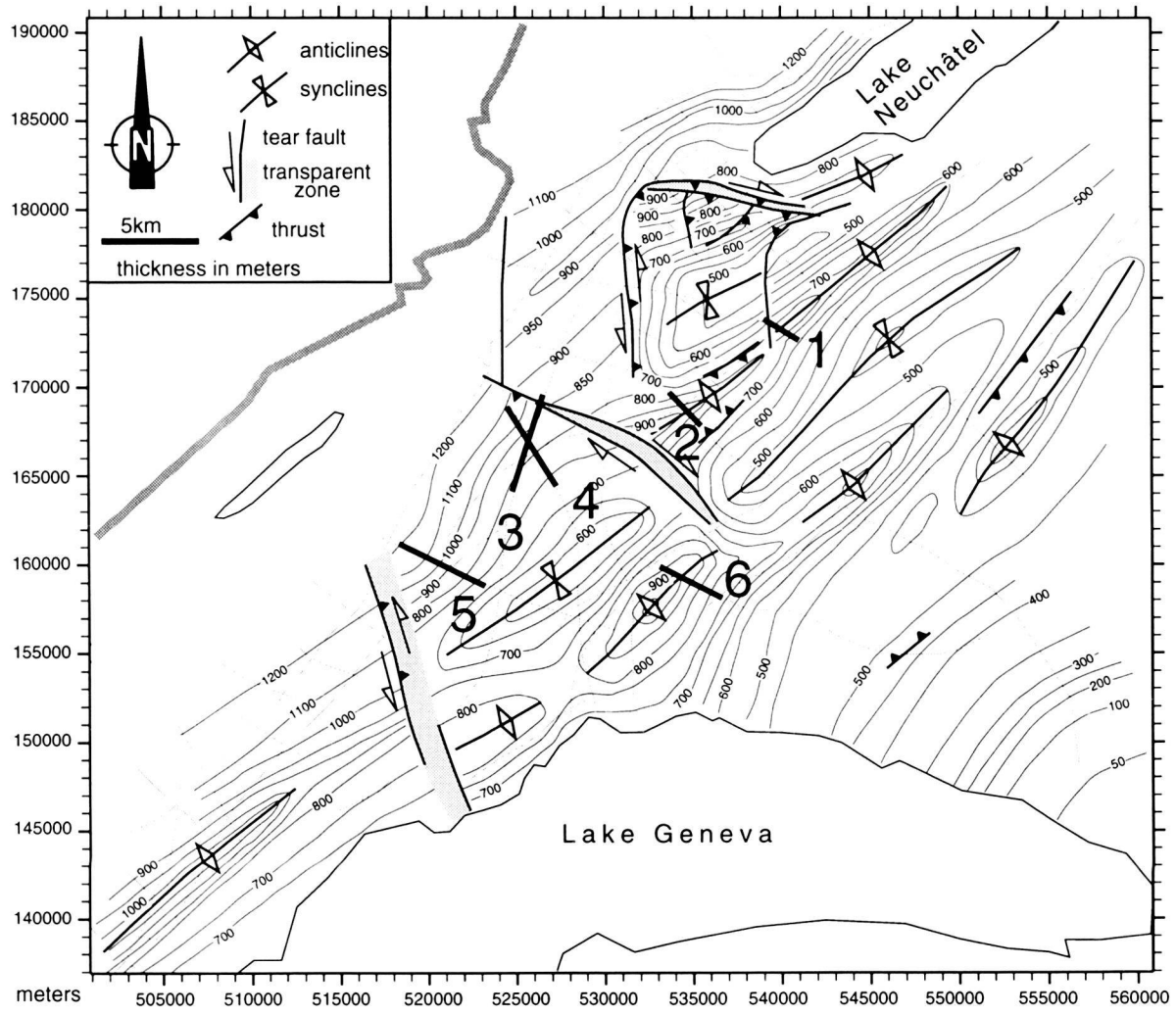

Figure 3.6: Isopach map of the Triassic Unit 2 beds from the western Molasse Basin (hand contouring). Compare with Figure 2.29. Anticline axes emphasize thick zones, syncline axes show thin zones. Location of six examples (Figs. 3.7 to 3.12) of evaporite stacks in the Triassic Unit 2. Coordinates in meters are according to the Swiss geographic reference grid. Modified from SOMMARUGA (1995).

Carte des isopaches de l'Unité 2 des couches du Trias du Bassin molassique occidental. Méthode de contourage à la main, comparer avec la Figure 2.29. Les axes des anticlinaux indiquent les zones très épaisses, les axes des synclinaux soulignent les zones peu épaisses. Localisation de six exemples (Figs. 3.7 à 3.12) d'empilements d'évaporites dans l'Unité 2 du Trias. Les coordonnées en mètres correspondent à la grille de référence géographique de la Suisse. Modifié de SOMMARUGA (1995).

3.2.2.4. Interpretation of the evaporite anticlines or pillows

The kinematic sequences in the central Jura and the Molasse Basin lines can be recognized on a number of examples of evaporite anticlines (Fig. 3.5 and Figs. 3.7 to 3.12).

Broad folds from the Plateau Jura and the Molasse Basin show in their core, thickening of evaporites, salt and clays within the Triassic Unit 2 (Panel 10 and Panel 5), which result in folding of the overlying layers. However, the Cretaceous, Jurassic and Triassic Unit 1 intervals maintain an apparently more constant thickness. Maybe because the seismic data are not of high quality, especially in the Plateau Jura, no truncations are visible within these strata. In some dip lines, located in the southern Molasse Basin e.g. Section 43 on Panel 5, Tertiary sediments onlap clearly the underlying strata. Onlaps have been observed mostly on south dipping limbs.

The interpretation of these onlaps is not clear. On the one hand, these onlaps may be due to salt flow to the NW and may thus be interpreted as evidence of salt movements since the beginning of Cenozoic time. To confirm this hypothesis, however, there

should be some onlaps onto North dipping limbs (there is only one case on strike Section 26, where onlaps are recognized to the SW). No onlap has been found on a north dipping limb, however. On the other hand, updip truncations toward the foreland may be interpreted as the foredeep unconformity. This major unconformity was induced by the subduction of the distal part of the European plate (BALLY, 1989, see also Chapter 5). This second hypothesis appears the most likely. In the central Jura and Molasse Basin, the Mesozoic layers, with the Oligocene and early Miocene sediments represent the prekinematic sequence. No synkinematic series has been observed on seismic lines. Evaporite flow was most likely contemporaneous to the main deformation, of late Miocene age in the Jura (LAUBSCHER, 1961). No evidence for growth anticlines, involving deposition of Tertiary Molasse sediments, has been found so far in the Jura or the Molasse Basin.

The detailed internal structure of swells within Triassic Unit 2 is unknown, since few evaporite-related anticlines have been drilled (Laveron, Essertines) and most other wells do not reach the Triassic Unit 2. In the Jura and Molasse Basin, the evolution stage is similar for all broad anticlines and it is thus difficult to describe the evolution of the deformation. Salt flow and/or stacking of thrust sheets (duplexes) are possible explanations for the observed swells.

True salt flow producing the so called salt pillows or salt anticlines is not really proven in the Jura fold and thrust belt, nor in the Molasse Basin. The Laveron stratigraphic well log, which shows more than 300 m of pure salt in Triassic layers, is the thickest pillow observed in the studied area and salt flow seems a reasonable assumption to explain this pillow (Fig. 3.5). The Triassic Unit 2 interval shows either discontinuous reflectors parallel to the overlying strata or no reflectivity (transparent zone). The reflectors do not highlight any structural relationships. The thick amount of salt and the absence of structural features suggest that the thickening within the Triassic Unit 2 is indeed the result of an accumulation of salt and evaporite by lateral flow. This flow occurs in a compressional regime and is not to be confused with conventional salt diapirism, which often occurs in an extensional context. It is important to underline, however, that no salt diapir has been observed, to date, in the Jura belt and the Molasse Basin. This is probably due the scarcity and thinness of pure rock salt layers present in the Triassic.

Low amplitude anticlines related to salt welts (see 3.2.2.1.) are well illustrated by HARRISON & BALLY (1988) and HARRISON (1995) on high quality seismic data from the Parry Islands Fold Belt (Melville Island, Canadian Arctic, Fig. 3.13). The increasing intensity of deformation toward the hinterland can be viewed as representing progressive stages of deformation and, as result, gives insight into the evolution of deformation within large anticlines. The first stage illustrates a salt welt, i.e. a significant triangular disharmony in the salt layer overlying the less disturbed unit. The triangular envelope of this salt welt is made of decoupling surfaces. In common language (BALLY, oral communication), this structure has been called "Napoleon's hat", due to the strong similarity in shape. With increasing shortening, the competent layers overlying the ductile zone respond by brittle behavior and the incompetent shales respond by flow (shale welt). The response to deformation varies, both laterally and vertically in the strata, as a function of the distribution of detachment levels and the relative thickness and competence of different formations. In the Melville Island case, thrust faults appear to be progressively younger from bottom to top. In comparison, the Jura Plateau and the Molasse Basin folds seem to be less evolved, since no obvious wedging is observed above the salt welts.

In the Molasse Basin, many broad anticlines present structural features within the Triassic Unit 2 layer (best examples are in Fig. 3.8 and Fig. 3.12). Strong reflectors dipping toward the South crosscut the whole unit. These can be interpreted as small imbricate thrust faults linking the floor thrust to the roof thrust (below reflector H). According to the classification of BOYER & ELLIOT (1982), these structures may correspond to hinterland dipping duplexes within an anticlinal core. These structures, confined to the lower unit just above the basement, result in folding of the mainly unfaulted overlying layers. The roof thrust of the duplex (just below reflector H) separates two different styles of deformation: the overlying layers are folded, whereas the underlying are faulted (thrusts) and/or ductily deformed.

In the Appalachian Plateau (Pennsylvania), MITRA (1986) presents a seismic line example of a duplex in the core of a major anticline (Fig. 3.14). The Lower to Upper Devonian units are folded into a broad unfaulted anticlinal arch. The Middle Ordovician carbonates (Trenton Formation) are affected by a series of imbricate thrusts that constitute a duplex. Additional thickening occurs within

the Upper Ordovician to Silurian units, but no reflectors are visible, due to the poor quality of the seismic lines. The basal Cambrian unit is not affected by the deformation. Imbricate thrust systems of this sort, have attracted much interest among petroleum geologists, since they constitute potential hydrocarbon traps.

In the eastern Jura, seismic sections show also important thickening within Triassic strata, as shown in the strike line presented on Figure 3.15. This seismic line crosses a low amplitude anticline (Born anticline), which is surrounded by Tertiary Molasse sediments. Beneath the broad anticline, the layer thickness increases between the reflectors representing the base of the Mesozoic and the top of the Muschelkalk (in gray color on Figure 3.15). This interval corresponds to the Triassic Unit 2 of the central Jura. This anticline is located between the Haute Chaîne Jura (Folded Jura) and the Plateau Molasse unit. The structural style of this evaporite-related anticline may be compared to the examples of the Figures 3.10 and 3.11, located in the most internal part of the folded Jura.

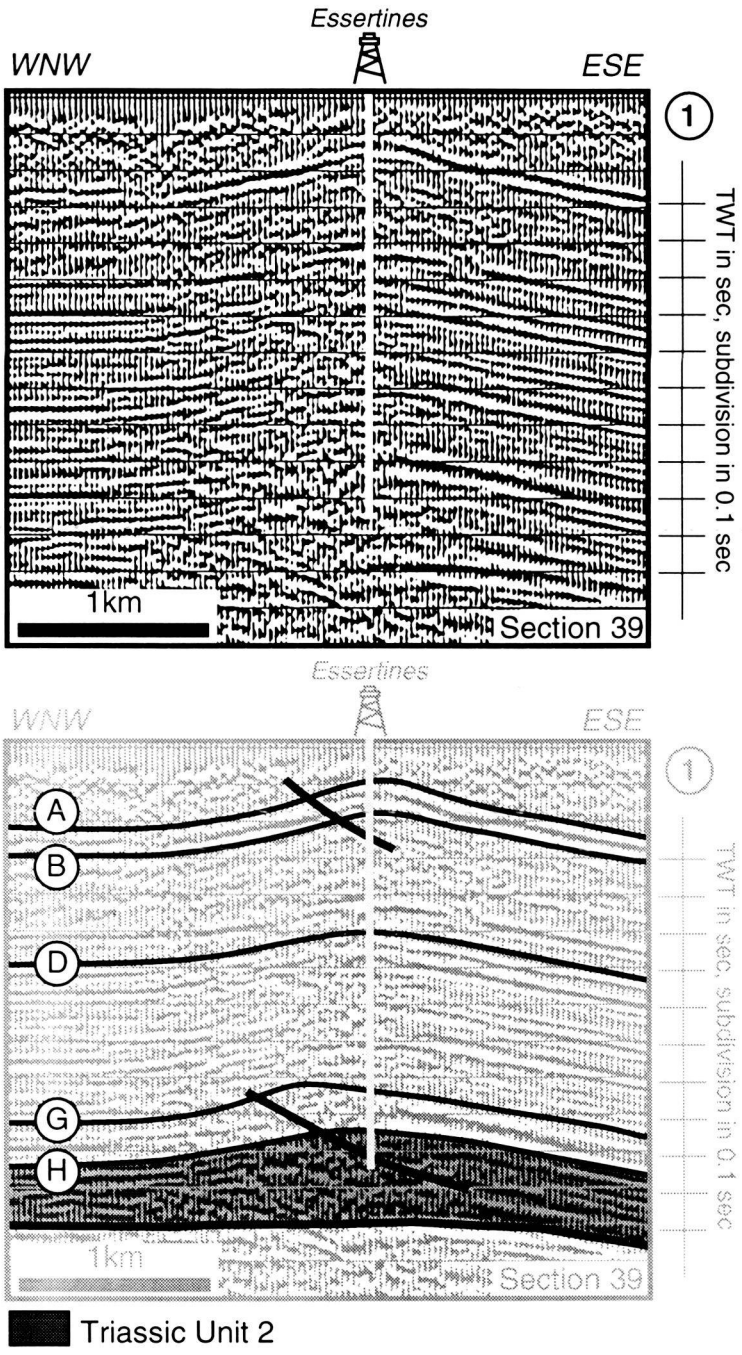

Figure 3.7: Southern part of the dip seismic Section 39 from the western Swiss Molasse Basin. For location, see example 1 on Figure 3.6. The interpretation, calibrated on the Essertines drill hole, shows a low amplitude fold related to a thickening within the Triassic Unit 2. Legend for the top of the layers: A = Lower Cretaceous or base Tertiary; B = upper Malm; D = Dogger; G = Triassic Unit 1, H = Triassic Unit 2.

Partie méridionale du profil sismique 39 transversal, situé dans le Bassin molassique suisse. Pour la localisation, voir exemple 1 sur la Figure 3.6. L'interprétation, calibrée sur le forage d'Essertines, montre un pli de faible amplitude associé à un épaississement dans les couches de l'Unité 2 du Trias. Légende pour le toit des couches: A = Crétacé inférieur ou base du Tertiaire; B = Malm supérieur; D = Dogger; G = Unité 1 du Trias, H = Unité 2 du Trias.

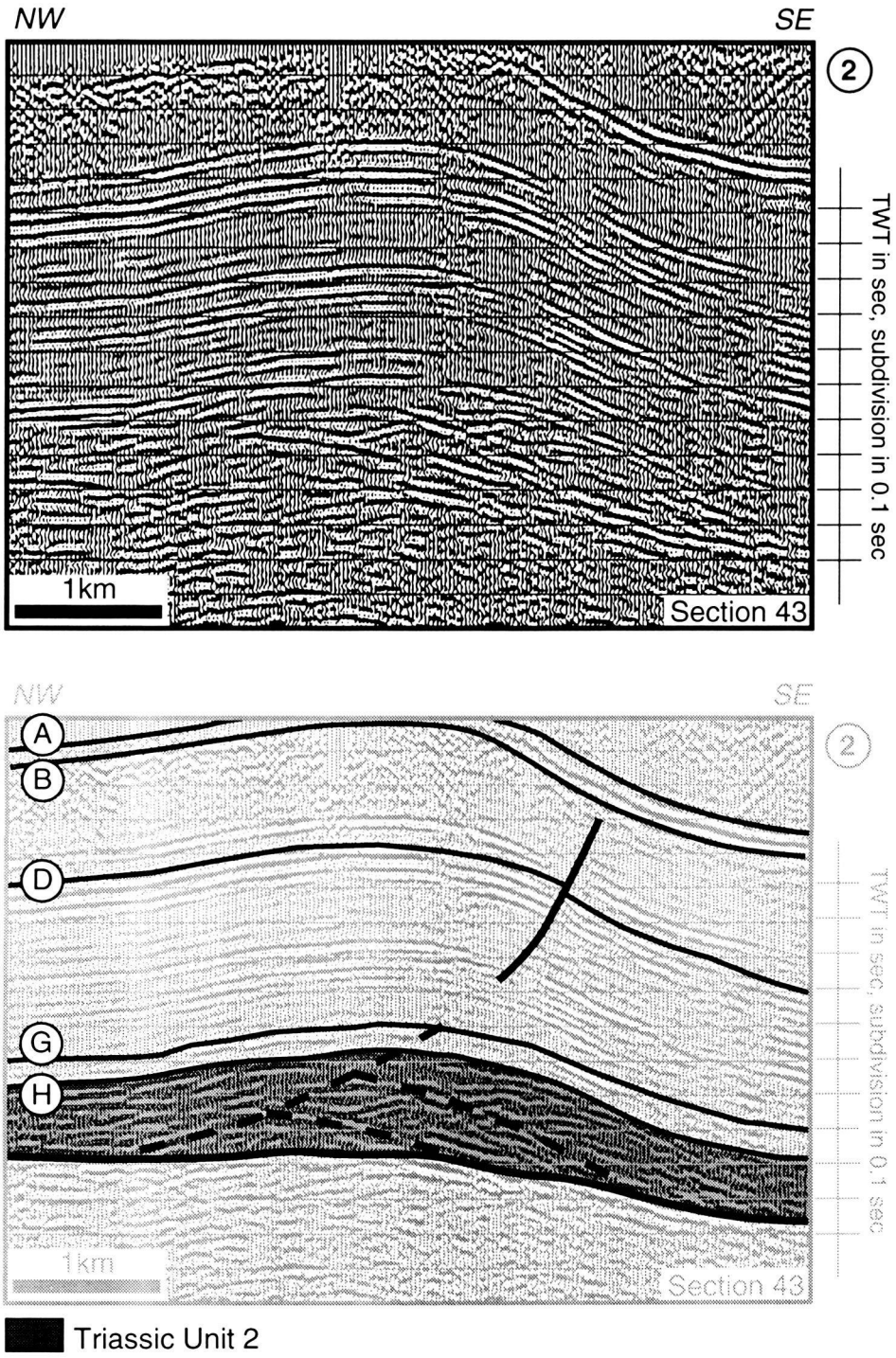

Figure 3.8: Northern part of the dip seismic Section 43 from the western Swiss Molasse Basin. For location, see example 2 on Figure 3.6. The interpretation shows a hinterland-vergent fold related to a thickening within the Triassic Unit 2. The thickening may be due to duplex structures. Legend for the top of the layers: A = Lower Cretaceous or base Tertiary; B = upper Malm; D = Dogger; G = Triassic Unit 1, H = Triassic Unit 2.

Partie septentrionale du profil sismique 43 transversal, situé dans le Bassin molassique suisse. Pour la localisation, voir exemple 2 sur la Figure 3.6. L'interprétation montre un pli à vergence vers le Sud, associé à un épaississement dans les couches de l'Unité 2 du Trias. L'épaississement est probablement dû à des structures imbriquées en duplex. Légende pour le toit des couches: A = Crétacé inférieur ou base du Tertiaire; B = Malm supérieur; D = Dogger; G = Unité 1 du Trias, H = Unité 2 du Trias.

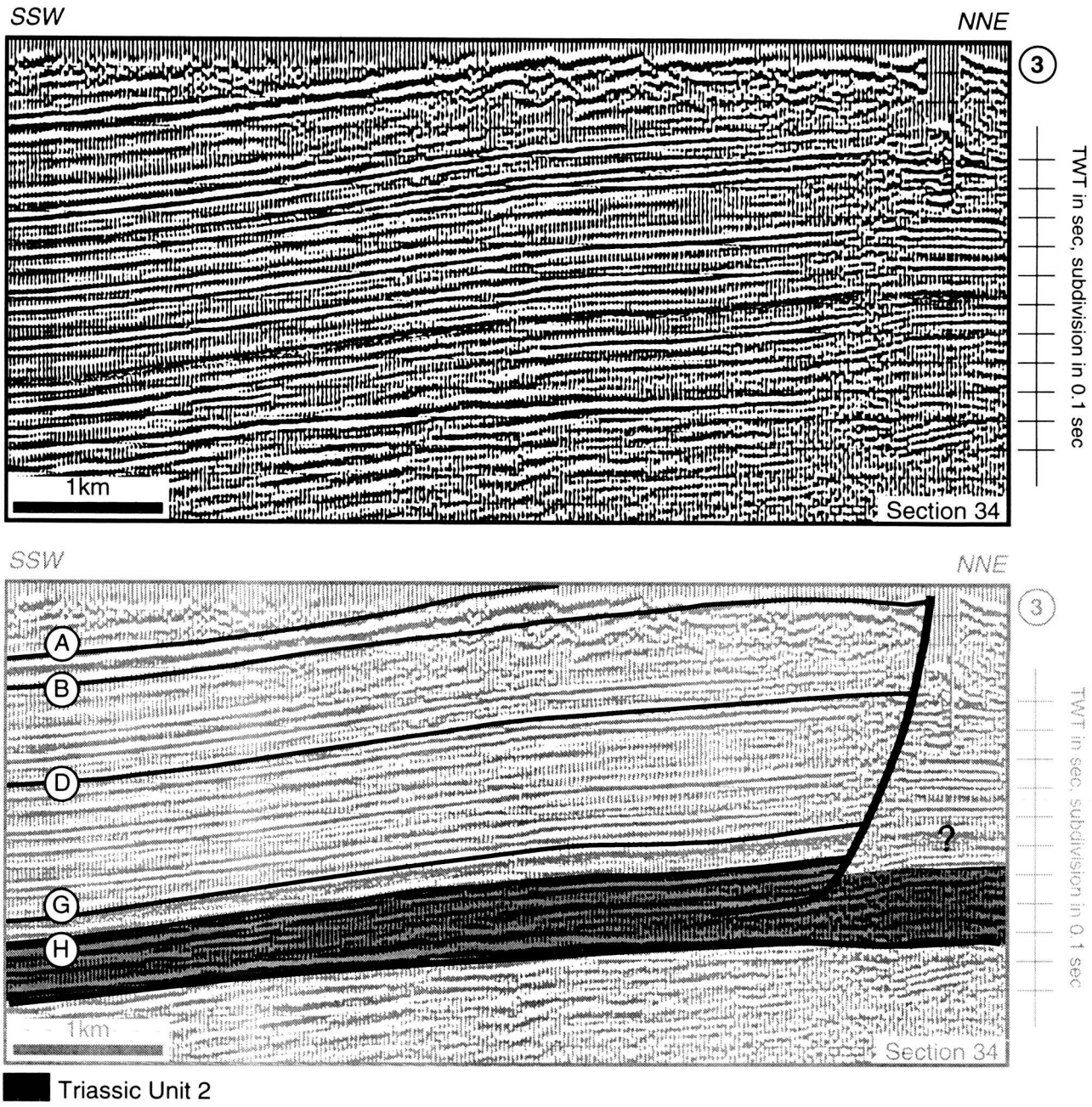

Figure 3.9: Southern part of the seismic Section 34 from the western Swiss Molasse Basin. For location, see example 3 on Figure 3.6. The interpretation shows a foreland-vergent fold related to a thickening within the Triassic Unit 2. A tear fault crosscuts the evaporite anticline (compare map of Figure 3.6). Legend for the top of the layers: A = Lower Cretaceous or base Tertiary; B = upper Malm; D = Dogger; G = Triassic Unit 1, H = Triassic Unit 2.

Partie méridionale du profil sismique 34, situé dans le Bassin molassique suisse. Pour la localisation, voir exemple 3 sur la Figure 3.6. L'interprétation montre un pli à vergence vers l'avant-pays, associé à un épaississement dans les couches de l'Unité 2 du Trias. Un décrochement recoupe l'anticlinal (comparer avec la carte de la Figure 3.6). Légende pour le toit des couches: A = Crétacé inférieur ou base du Tertiaire; B = Malm supérieur; D = Dogger; G = Unité 1 du Trias, H = Unité 2 du Trias.

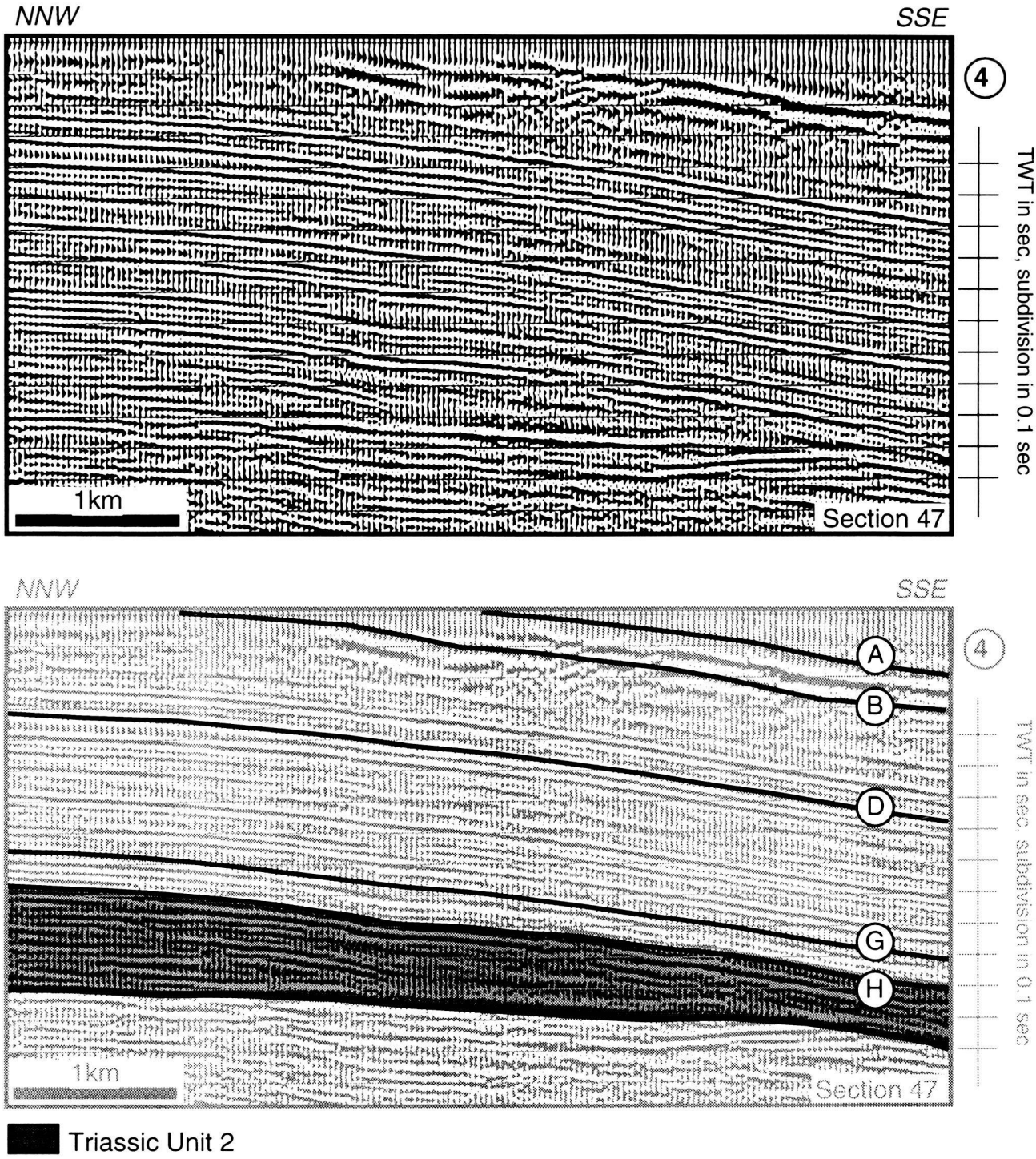

Figure 3.10: Northern part of the dip seismic Section 47 from the western Swiss Molasse Basin. For location, see example 4 on Figure 3.6. The interpretation shows a foreland-vergent fold related to a thickening within the Triassic Unit 2. Legend for the top of the layers: A = Lower Cretaceous or base Tertiary; B = upper Malm; D = Dogger; G = Triassic Unit 1, H = Triassic Unit 2.

Partie septentrionale du profil sismique 47 transversal, situé dans le Bassin molassique suisse. Pour la localisation, voir exemple 4 sur la Figure 3.6. L'interprétation montre un pli à vergence vers le NW, associé à un épaississement dans les couches de l'Unité 2 du Trias. Légende pour le toit des couches: A = Crétacé inférieur ou base du Tertiaire; B = Malm supérieur; D = Dogger; G = Unité 1 du Trias, H = Unité 2 du Trias.

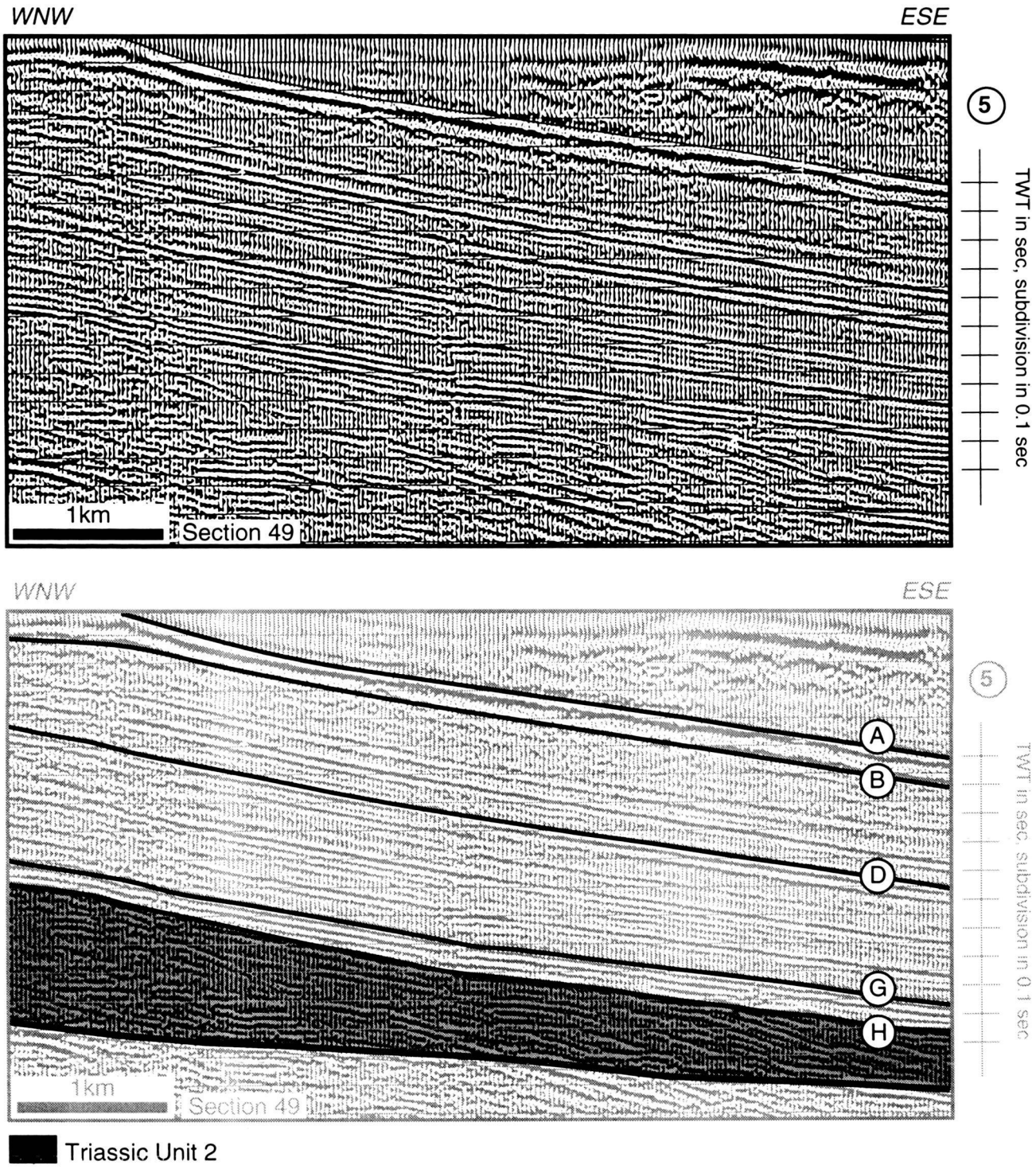

Figure 3.11: Northern part of the dip seismic Section 49 from the western Swiss Molasse Basin. For location, see example 5 on Figure 3.6. The interpretation shows a foreland-vergent fold related to a thickening within the Triassic Unit 2. The thickening may be due to duplex structures. Legend for the top of the layers: A = Lower Cretaceous or base Tertiary; B = upper Malm; D = Dogger; G = Triassic Unit 1, H = Triassic Unit 2.

Partie septentrionale du profil sismique 49 transversal, situé dans le Bassin molassique suisse. Pour la localisation, voir exemple 5 sur la Figure 3.6. L'interprétation montre un pli à vergence vers le Nord, associé à un épaississement dans les couches de l'Unité 2 du Trias. L'épaississement est peut-être dû à des structures imbriquées en duplex. Légende pour le toit des couches: A = Crétacé inférieur ou base du Tertiaire; B = Malm supérieur; D = Dogger; G = Unité 1 du Trias, H = Unité 2 du Trias.

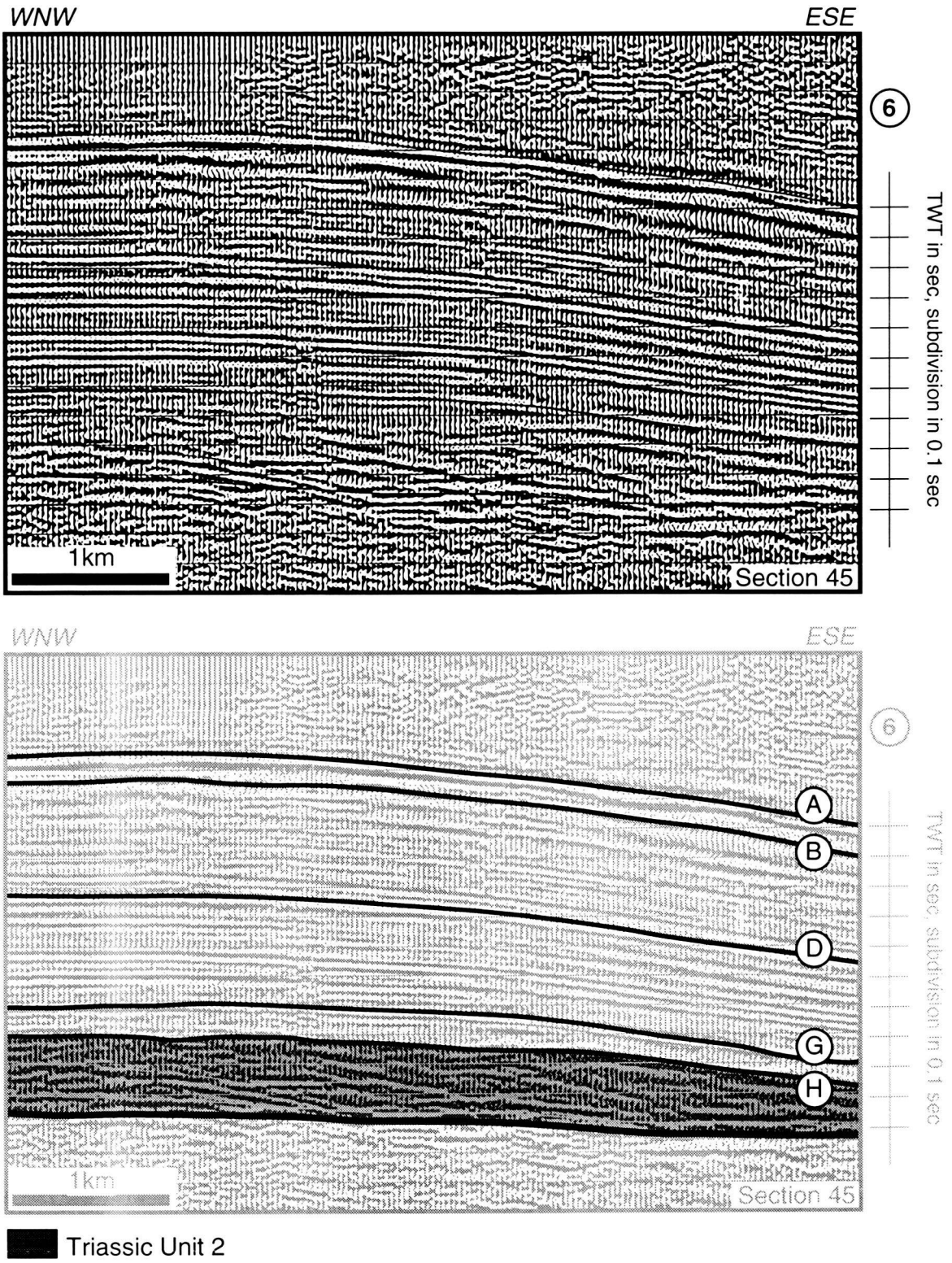

Figure 3.12: Northern part of the dip seismic Section 45 from the western Swiss Molasse Basin. For location, see example 6 on Figure 3.6. The interpretation shows a foreland-vergent fold related to a thickening within the Triassic Unit 2. The thickening may be due to duplex structures. Legend for the top of the layers: A = Lower Cretaceous or base Tertiary; B = upper Malm; D = Dogger; G = Triassic Unit 1, H = Triassic Unit 2.

Partie septentrionale du profil sismique 45 transversal, situé dans le Bassin molassique suisse. Pour la localisation, voir exemple 6 sur la Figure 3.6. L'interprétation montre un pli à vergence vers l'avant-pays, associé à un épaississement dans les couches de l'Unité 2 du Trias. L'épaississement est peut-être dû à des structures imbriquées en duplex. Légende pour le toit des couches: A = Crétacé inférieur ou base du Tertiaire; B = Malm supérieur; D = Dogger; G = Unité 1 du Trias, H = Unité 2 du Trias.

a)

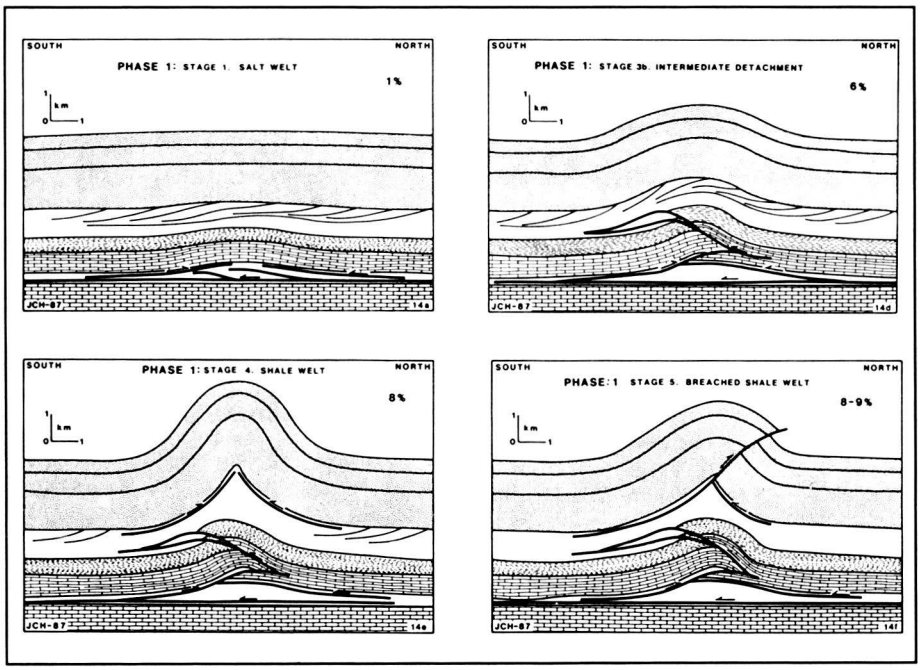

From Harrison & Bally (1988)

b)

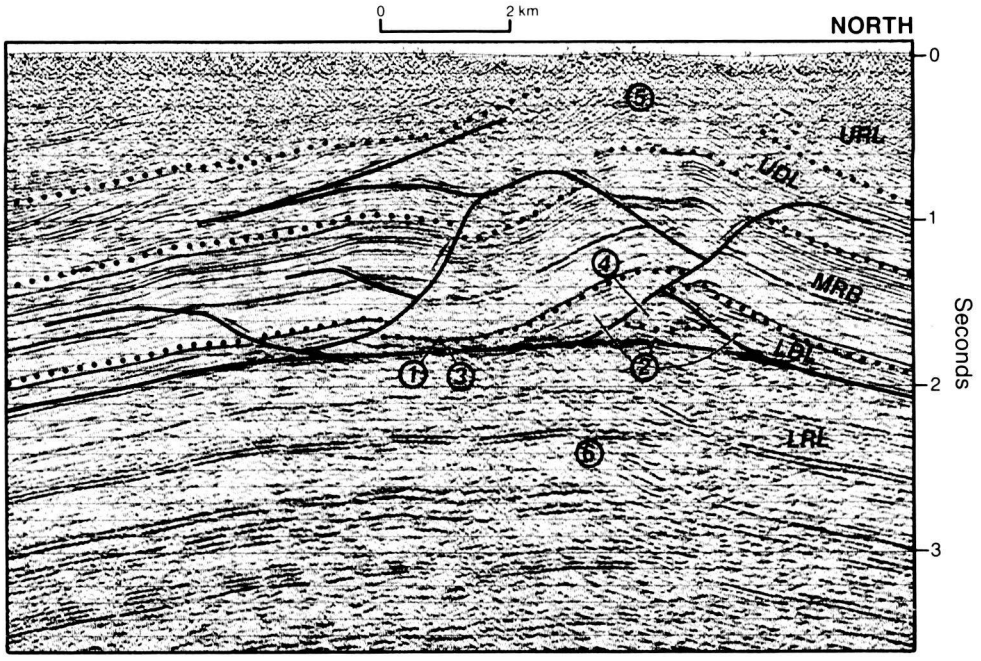

From Harrison (1995)

Figure 3.13:
a) Stages from the evolution of an anticline in the salt-based Parry Islands Fold Belt (Melville Island). Modified from HARRISON & BALLY (1988).

Evolution d'un anticlinal dans la chaîne plissée de l'île de Melville (territoires arctiques). Modifié de HARRISON & BALLY (1988).

b) Example of an anticline from Melville Island. LRL = lower rigid layer; LDL = lower ductile layer; MRB = medial rigid beam; UDL = upper ductile layer; URL = upper rigid layer; 1 = footwall syncline; 2 = a compound anticlinal salt welt with a faulted and indistinct hinge saddle; 3 = dramatic local thinning of the lower Bay beam is encapsulated by evaporites; 5 = some anticlinal hinge thickening of mud rock is indicated for the Cape de Bray formation; 6 = the crest of structures at deeper level. From HARRISON (1995, Figure 123).

Exemple d'un anticlinal de l'île de Meville. LRL = couche rigide inférieure; LDL = couche ductile inférieure; MRB = niveau rigide moyen; UDL = couche ductile supérieure; URL = couche rigide supérieure; 1 = synclinal dans le mur; 2 = anticlinal composite avec une charnière faillée en forme de selle; 3 = important amincissement du niveau "lower Bay" enveloppé par des évaporites; 5 = un faible épaississement de la charnière par des roches argileuses est montré pour la formation du Cape de Bray ; 6 = crête des structures localisées à un niveau inférieur. Tiré de HARRISON (1995, Figure 123).

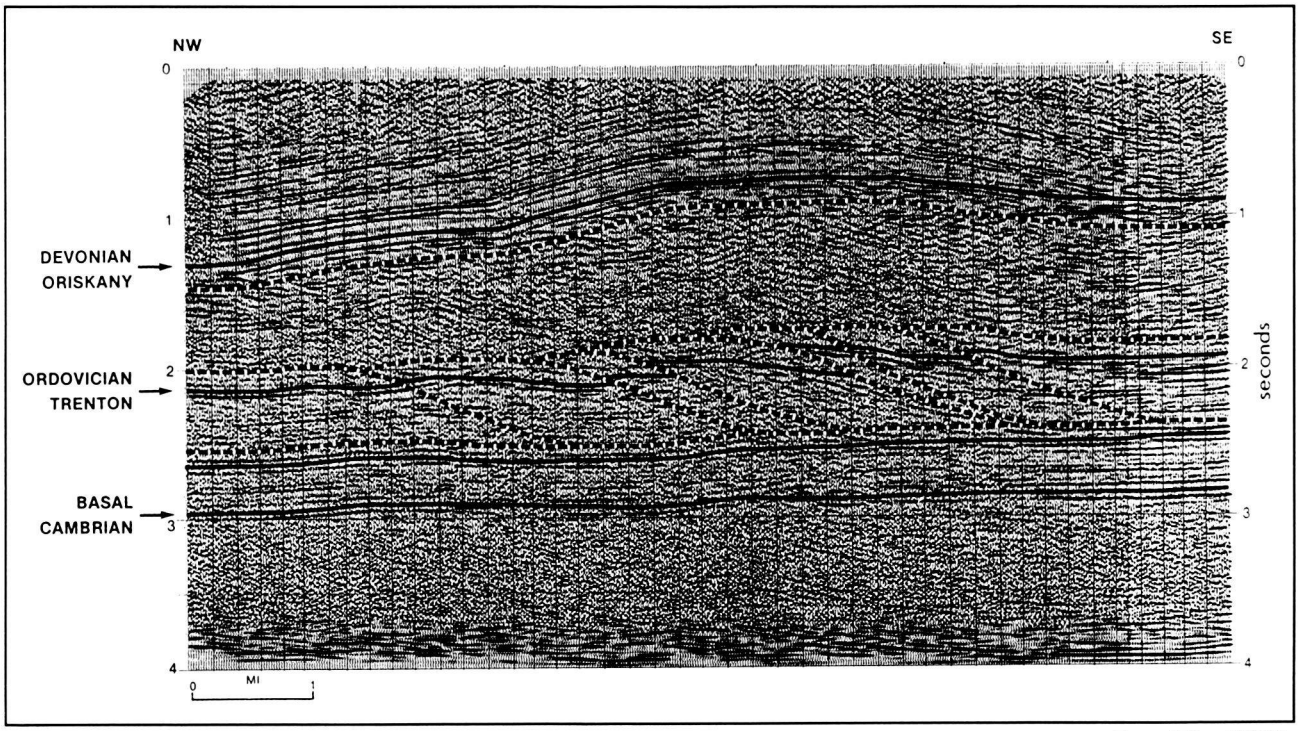

From Mitra (1986)

Figure 3.14: Migrated seismic profile across an anticline in the Appalachian Plateau (Pennsylvania). Devonian units are folded into a broad anticlinal arch cored by duplexes in Ordovician carbonates. Interpretation and figure are from MITRA (©1986, Figure 27, reprinted by the permission of the "American Association of Petroleum Geologists").

Profil sismique migré d'un anticlinal du Plateau appalachien (Pennsylvanie). Les unités du Dévonien forment une large arche anticlinale, remplie par des imbrications en duplex dans les carbonates de l'Ordovicien. L'interprétation et la figure sont tirées de MITRA (©1986, Figure 27, reproduite avec la permission de l'"American Association of Petroleum Geologists").

Concluding on the evaporite-related folds, it is suggested that the broad anticlines from the Plateau Jura are related to salt flow within the Triassic Unit 2, whereas Molasse Basin anticlines are related to well organized evaporite duplexes within the Triassic Unit 2. This difference is probably related to mineralogical composition and hence to the rheology of the Triassic evaporites. In the northern parts, considerable amounts of pure salt seem to be present within this formation, whereas in the southern parts its presence is not yet proven. Duplexes seem to have formed within the slightly more competent Triassic Unit 2 of the Jura internal parts and of the Molasse Basin.

In the preceding paragraphs, the geometry and the kinematics of evaporite pillows have been discussed. In terms of mechanism, buckling seems the most adequate for the observed structural style and rheology. The Triassic Unit 2, which consists of salt, evaporite and clay rocks, has a low viscosity in comparison with the overlying alternating carbonate and shale layers. These rheological conditions favor folding by flexural-flow. The weakest layer, Triassic Unit 2 (see Figure 2.30), flows into the core of the anticline presenting thickening of the unit, whereas the strong layers buckle without any thickness changes (concentric folds).

3.2.3. Thrust-related folds (high amplitude)

3.2.3.1. General comments

The sinusoidal shape of the Jura folds drawn by earlier geologists e.g. in DE MARGERIE (1922), HEIM (1921), RICKENBACH (1925), SUTER & LÜTHI (1969) (see Chapter 4 Regional geology) has been shown to be an oversimplification, not only in the central Jura, but also in the eastern (LAUBSCHER, 1977) and western Jura (PHILIPPE, 1994). In most places, at the surface, a veneer of Quaternary sediments obscures the critical relationships between strata and thrust faults. Seismic data have, however, confirmed that folds are related to major thrust faults. This relationship has been already suggested by different authors in the eastern and western part of the Jura (BUXTORF, 1916; LAUBSCHER, 1985; DIEBOLD *et al.*, 1991; PHILIPPE, 1994).

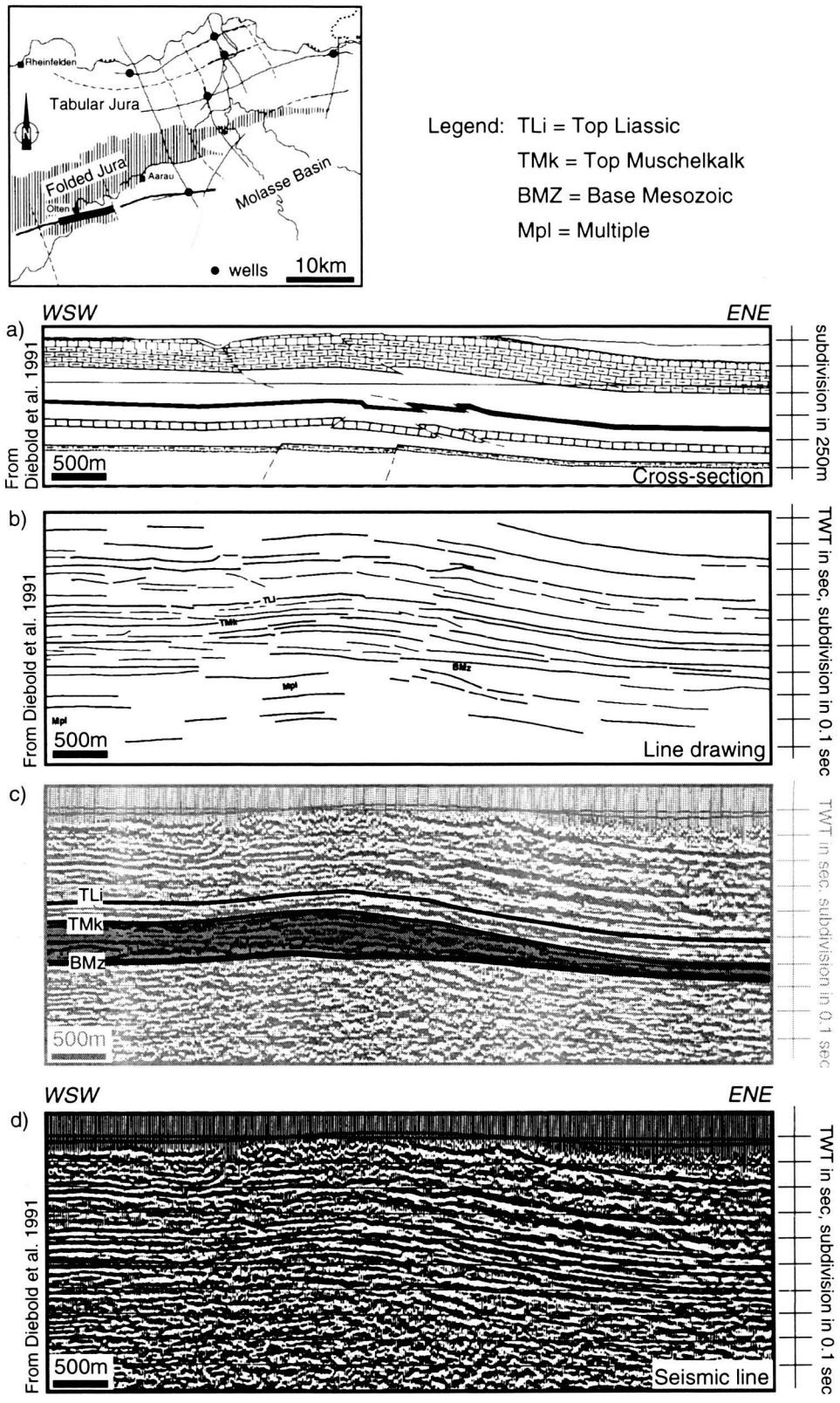

Figure 3.15: Strike seismic line from the Nagra work located in the eastern Jura (southern side). a) Geological cross-section. b) Line drawing of the seismic section. c) Interpretation of the seismic line. "Muschelkalk" layers, highlighted in gray, present a thickening (evaporite pillow) beneath the broad anticline. d) Seismic profile. The location is shown on the map. The seismic line, the line drawing and the cross-section are from DIEBOLD *et al.* (1991).

Profil sismique longitudinal et coupe géologique localisés dans le Jura oriental (partie méridionale). a) Coupe géologique. b) Réflecteurs du profil sismique. c) Interprétation du profil sismique. Les couches du "Muschelkalk", soulignées en gris, montrent un épaississement (coussin d'évaporites) sous le large anticlinal. d) Profil sismique, voir localisation sur la carte. Le profil sismique, le dessin et la coupe géologique sont tirés de DIEBOLD *et al. (1991).*

The observed scale of folding ranges from kilometers to meters. The first corresponds to large anticlines (regional scale), whereas the second consists of disharmonic folds, with metric wavelength (outcrop or minor scale). The latter are developed contemporaneously with the large scale structures. Disharmonic folding is observed between the stiff limestone beds and the weak marl layers (Fig. 2.30).

3.2.3.2. Geophysical evidence from seismic profiles

Generally the geophysical evidence for large subsurface thrusts includes duplication of coherent successions of seismic stratigraphic reflectors and velocity anomalies caused by tectonic duplication of strata higher in the section.

On many profiles, velocity anomalies are observed. The anomaly is usually a low positive deflection of the reflectors beneath anticlines (velocity pull-up) and a negative deflection beneath synclines (velocity pull-down). The dip Section 1 (Panel 1 and Plate 1) and Section 3 (Panel 1 and Plate 2) and the strike Section 8 (Panel 3 and Plate 3) from the Neuchâtel Jura illustrate such anomalies.

Recognition of repeated seismic stratigraphic reflections is the most common and evident form of identification of subsurface thrusts. Repetition, more obvious on lines parallel to the trend of the structures (strike lines), is one major reason for careful interpretation of seismic stratigraphy on strike lines. The lack of resolution often observed on dip profiles below the anticlines can be explained by many structural complications, but also by the steep topography. Strike Section 14 (Panel 3 and Plate 5) and dip Section 11 (Panel 2 and Plate 4) from the Neuchâtel Jura and strike Sections 80, 82 and 84 (Panel 8) and dip Sections 81, 83, 85, 87, 93 from the Risoux Jura document clearly duplication of reflectors. The Mt-Risoux anticline on Section 93 also shows duplication of the Jurassic series, confirmed by a well (WINNOCK, 1961) (Fig. 2.19).

3.2.3.3. Geometry of large scale folds illustrated by seismic profiles

Transverse lines crossing the Jura, oriented perpendicularly to the fold axes (NW-SE), allow to constrain of the fold geometry at depth. Line drawings of dip sections on panels 1, 2, and 9 illustrate the type of folds from the Haute Chaîne Jura (see Figure 1.2, for location on geological map). These high amplitude folds, which are asymmetric and are clearly related to thrust faults, root in the basal décollement zone located within the evaporites of the Triassic Unit 2. These thrust-related anticlines cause duplication of these Mesozoic stratigraphic layers. Thrust-related anticlines are separated by broad or tight synclines, Val de Ruz (Panel 1) and Val de Travers (Panel 2) respectively, which display flat lying, parallel layers.

Many thrust faults are NW (NNW) verging, like the main thrust system (foreland-vergent thrust). SE (SSE) vergent thrust faults are considered as backthrusts (hinterland-vergent thrusts). Thrust faults include both flats and ramps, e.g. Section 1 on Panel 1 or Plate 1, Sections 11 (Nouvelle Censière anticline, Plate 4, see also Fig. 4.7b), 13, 17 on Panel 2 (Neuchâtel Jura) and Sections 85, 111 (Mt-Risoux anticline, Plate 8), 95 on Panel 9 (Vaud and France Jura). In the flats, thrust faults are parallel to the overlying layers or parallel to the main décollement plane, whereas, in the ramps, the thrust fault cuts across the layers. All seismically mapped thrust faults are throughgoing to the surface, breaking through the structures in the steep frontal limbs e.g. Sections 1, 3 on Panel 1 and Section 11 on Panel 2. The leading edge of the thrust sheet may also show some imbrications e.g. Sections 5 and 7 on Panel 1.

Many backthrusts are associated with foreland-vergent thrust faults. They seem to be localized in kink or steep dip data zones, identified on geological maps e.g. Section 3 on Panel 1, Sections 11, 13, 17 on Panel 2 and Section 111 on Panel 9, but also appear to be connected to a main thrust fault at the transition between a flat and a ramp portion. Foreland-vergent thrusts have a kilometric dipslip displacement (e.g. Section 11 on Panel 2 and Section 111 -southern part- on Panel 9) and hinterland-vergent thrusts generally have few tens or hundreds of meters of displacements. Sometimes, as in the backthrust of the Mt-Risoux anticline (Sections 85, 111 -southern part- on Panel 9), a kilometric displacement can be observed.

The foreland-vergent thrust ramps have step-up angles between 20° and 30° (sometimes more), whereas backthrusts in the Neuchâtel Jura are much steeper (±60°) or else much shallower, as in the Vaud Jura (Mt-Risoux, Sections 85 and 111, southern part). These angles are approximate, because they are deduced from the seismic interpretations, which are displayed in TWT (seconds).

The Triassic Unit 2 evaporite layers are considered as the major regional décollement zone. The thrust ramps of the anticlines described above, root in this zone. Triassic Unit 2 layers appear very thick on the seismic lines (see line drawings on panels and Figure 2.30 of §2.6.). Formations beneath this very weak zone represent the basement. The term basement includes any rocks or sediments not involved in the formation of the overlying folds. The top of the basement appears as a smooth and flat surface dipping 1° to 3° to the S-SE (Fig. 5.1).

Some smaller scale thrust-related folds, e.g. the example of Figure 3.16, have a main thrust fault that roots in the lower Malm layers ("Argovian facies"). This figure is a dip line, located at the southwestern edge of the studied area, that crosses the transition from the Molasse Basin to the Jura Haute Chaîne. The thrust fault on this seismic line (Section 71, Fig. 3.16) is clearly documented by numerous flat reflectors (between B and C reflectors) cut by south-dipping reflectors. Unfortunately, this is the only example documented on seismic lines of the study area. Such minor scale folds are, however, already well known from surface geology (DROXLER, 1978; PFIFFNER, 1990) and will be discussed later.

In conclusion, the new seismic data confirm that large scale anticlines are formed above NNW vergent thrusts with kilometric dipslip displacement. Important thrusting results in duplication of the entire Jurassic stratigraphic sequence. These thrusts root in the basal décollement zone located in the evaporites of the Triassic Unit 2, which are surprisingly thick and clearly involved in the thrusting.

3.2.3.4. Minor scale deformation and disharmonic folds illustrated by outcrops

At the outcrop scale, deformation is brittle, characterized by stylolites, veins and small faults bearing slickensides. Deformation is localized within fold hinges and narrow fractured zones separating seemingly undeformed regions (limbs). Construction of a pilot tunnel below La Vue des Alpes (between the cities of Neuchâtel and La Chaux de Fonds, eastern Neuchâtel Jura, (Figs. 4.3 and 4.5) allowed Xavier Tschanz (from Neuchâtel University) to observe subsurface outcrops along a continuous profile of an anticline from the Neuchâtel Haute Chaîne Jura. This profile, running perpendicular to the fold axis and located along the same trace as the seismic Section 3 (Panel 1 and Plate 2), is more or less between intersections 4 and 2. Results from observation of fresh outcrops in the drilled tunnel are discussed in more detail in the paper by TSCHANZ & SOMMARUGA (1993). The rocks displayed surprisingly few deformation features. Vein volumes generally represent less than c.a. 0.5% of the rock and very few tectonic stylolites are present. The more intense deformations occurred only within sharp kink and hinge zones. These are characterized by an increased number of seemingly chaotic calcite veins, representing in places up to about 5% of the total rock volume. Locally, reverse and normal faults with a decimetric throw were identified. Meter scale offset faults are associated to the major kink and hinge zones. On seismic Section 3 (on Panel 1, 2 km North of intersection 4), these zones are interpreted as related to a backthrust. Bedding parallel slip surfaces are present along the whole anticline. Stylolites, veins, striae and twins are the expression of strain at the outcrop and sample scale, respectively and demonstrate strains at scales smaller than the wavelength of the folds.

At sample scale, calcite twin strain analyses in bioclastic coarse grained Dogger limestones from the Neuchâtel Jura (Val de Ruz), revealed small intracrystalline deformations on the order of 1 to 4% shortening. All twins observed in this study are thin and straight (micro-)twins. These microstructures are indicative of minor deformation at very low temperatures (<<150°C) (GROSHONG *et al.*, 1984; BURKHARD, 1993). This local study can be integrated with the regional study of TSCHANZ (1990), which presents the same results analyzed on calcite twins from the whole central Jura.

Minor scale décollement levels, producing small scale folds, observed at the base of the lower Malm marls ("Argovian" facies) and the Cretaceous (Hauterivian) marls (see Figure 2.30) are discussed in two cases below.

A detailed study at the outcrop scale has been made by PFIFFNER (1990) in lower Malm limestone and shale interlayered beds (for rheology, see Figure 2.30) at the frontal hinge of a large scale, SE-vergent anticline (St-Sulpice, western edge of the Val de Travers syncline, Neuchâtel Jura, see Figure 4.3 for location on the map). Figure 3.17 shows several zoom sections at different scales. The geological cross-section (Fig. 3.17b), located halfway between seismic Sections 13 and 15 (Fig. 3.17a), has been modified from that of Pfiffner. Seismic data has improved the geometry at depth and the thickness of the Dogger, Liassic and Triassic units.

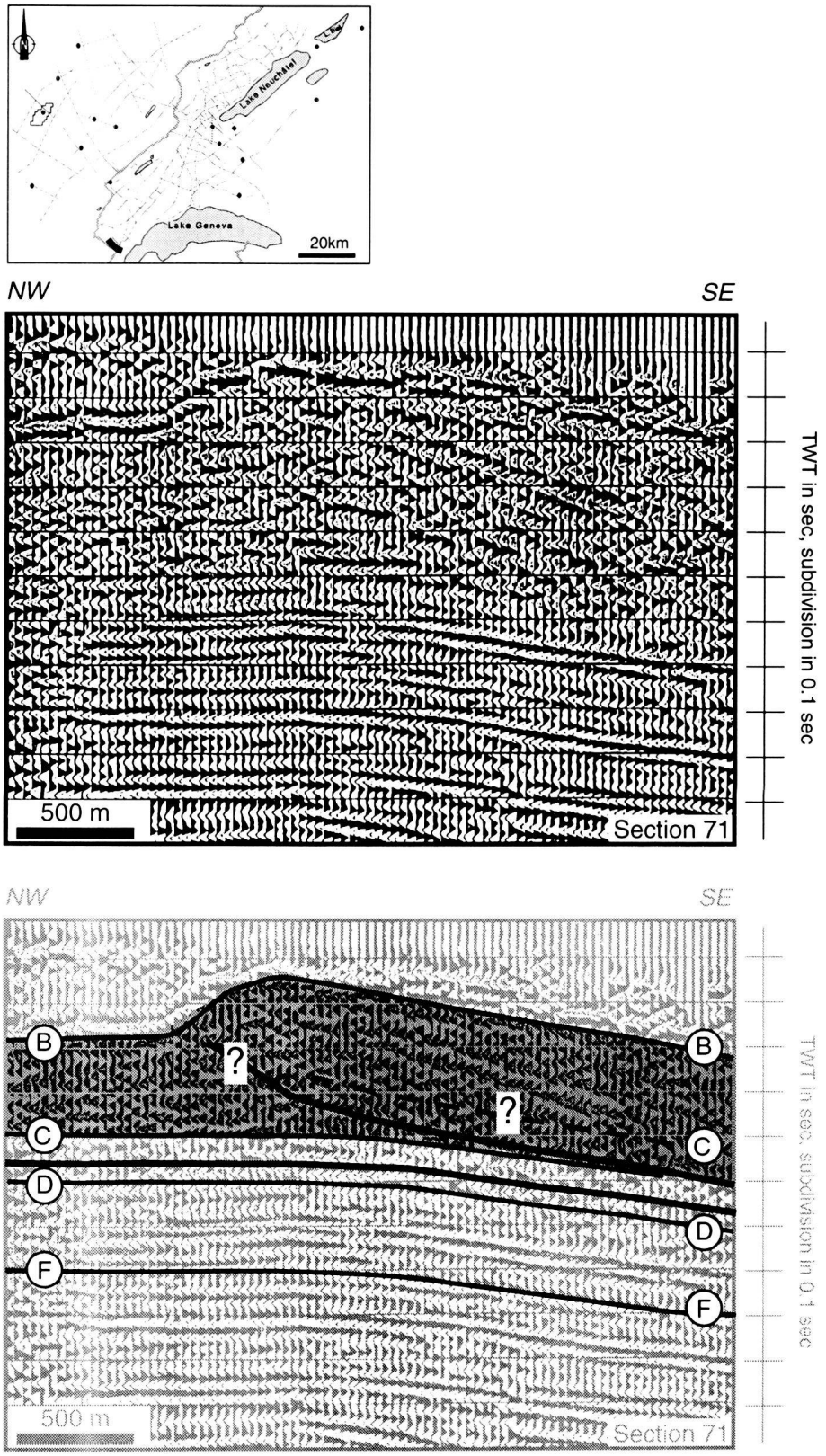

Figure 3.16: Portion of the dip seismic Section 71 located at the internal limit of the Jura Haute Chaîne. The interpretation shows a fold related to a thrust which roots in a minor décollement level at the base of the lower Malm unit ("Argovian" formation). Legend for the top of the layers: B = upper Malm; C = lower Malm; D = Dogger; F = Liassic.

Partie du profil sismique 71 transversal localisé à la limite interne de la Haute Chaîne jurassienne. L'interprétation présente un pli en relation avec un chevauchement qui s'enracine dans un niveau de décollement mineur à la base du Malm inférieur ("Argovien"). Légende pour le toit des couches: B = Malm supérieur; C = Malm inférieur; D = Dogger; F = Lias.

The seismic and geological sections show, at regional scale, a hinterland-vergent anticline related to a thrust fault, rooting in the main décollement level (Triassic Unit 2). The Val de Travers syncline shows two thrust faults in the Triassic units. This shortening is accommodated in the overlying layers by fish-tail structures. In the field, several disharmonic folds can be seen; these are of small wavelength and developed above a minor décollement level located in lower Malm shales ("Argovian") (Figs. 3.17c and 3.17d). According to PFIFFNER (1990, p.585), "individual limestone layers maintain compatibility within large scale structures by folding, bedding plane slip, conjugate contractional and extensional faults, and duplexes. The thickness of individual limestone layers appears not to be altered by a significant amount. Some of the contractional faults indicate considerable layer-parallel shortening in the early history of the folds. The ductile behavior indicated by round fold hinges is mainly linked to small scale faulting."

Metric and decimetric disharmonic folds are also common in the thin bedded limestones of the Lower Cretaceous (Hauterivian). A décollement level is present between the Cretaceous beds and the stiff Malm limestones, where strong disharmony in folding style is observed. Within the Cretaceous, décollement can also occur within the Hauterivian marls. The geometry and the kinematics of these folds have been analyzed in detail by DROXLER & SCHAER (1979) at one outcrop of the Neuchâtel Jura. According to these authors, ruptures induced by shearing and traction during the fold evolution have transformed the layers into semi-independent groups of fragments, the external geometry of which has been modified by dissolution in pressured zones. Part of the dissolved material in stylolitic planes is recrystallized in extension cracks.

These folds in the Cretaceous layers are attributed to Miocene thrusting e.g. in the Verrières syncline (Haute Chaîne Jura, France, Fig. 4.3) (MARTIN *et al.*, 1991), in contrast to the gravity sliding hypothesis ("collapse structure") suggested first by CASTANY (1947).

3.2.3.5. Interpretation of the thrust-related folds

In the Haute Chaîne Jura, high amplitude folds, though apparently simple, result from the superposition of a number of processes active at metric to kilometric scale. Stylolites, veins, striae and twins demonstrate strain at scales much smaller than the wavelength of the folds (§3.2.3.4).

Though the wavelength of the Haute Chaîne fold-geometry seems to be determined by the thickness of the Malm layers, the overall rheology of the sedimentary cover (see Figure 2.30) has an important influence on the shape of Jura folds. The thickness of the sedimentary cover decreases from SW towards NE, so that higher amplitude folds are located in the southwestern area (higher topographic relief in Canton Vaud, Canton Geneva and in France), whereas in the East topographic relief is much lower (Canton Aargau and Jura).

The presence of a thick, very weak sole layer, in contrast with more competent overlying layers, also determines the fold type. The very weak zone consists of evaporites, salt and clays (see description and discussion in §2.6.2) of the Triassic Unit 2 layers. This interval shows clearly thickness changes in the Plateau Jura and the Molasse Basin. In the central part of the Haute Chaîne, this interval appears to be thick and of constant thickness in some synclines (Val de Travers and Val de Ruz, Sections 4, 6, 8 on Panel 3). In the northern part of the Neuchâtel Jura however, the La Brévine syncline (Section 2 on Panel 3) shows duplication of the Triassic Unit 2 along the whole valley, which may explain the high elevation (1000 m) of this syncline, in comparison with the Val de Travers and Val de Ruz synclines (600 m to 800 m). The poor quality of seismic data beneath anticlines does not allow for accurate interpretation. Although the combination of the interpretation of several dip and strike lines (seismic grid) suggests that the Triassic Unit 2 interval is thick, in some cases this thickness results from an obvious tectonic duplication.

The sedimentary cover of the central Jura represents a multilayer sequence with a thick and particularly weak layer at the base of the sequence, corresponding to the décollement zone. The overlying layers consist of alternating marls (incompetent layer) and limestones (competent strong layers, Fig. 2.30). A high viscosity contrast also exists between the very weak Triassic Unit 2 layer and the weak to strong overlying layers. The Haute Chaîne Jura folds were initiated first as buckle folds in response to the layer-parallel compression. Evaporites, clays and salt rock infilled the space generated at the base of the sequence by inflowing mechanisms. These first stage buckle fold, also called detachment fold, then developed into fault-propagation folds and fault-bend folds after breakthrough of thrusts, with progressive deformation. The deformation within the stiff layers is accommodated mainly by bedding-

plane slip, pressure solution and brittle faulting. The Chaumont (southern anticline on Sections 1 and 3 on Panel 1) and SomMartel anticlines (Intersection 2 on Section 5, Panel 1) are examples of detachment folds that evolved into fault-propagation style folds. On the geological cross-section of Figure 4.5, located more or less parallel to the seismic Section 3, the Chaumont anticline presents a breakthrough in the steeper forelimb (see High-Angle Breakthrough in SUPPE & MEDWEDEFF (1990). The anticlines of the Nouvelle Censière (Section 11 on Panel 2) and the Mt-Risoux (Section 111-87 on Panel 9) are examples of detachment folds developed later over a ramp - flat geometry (fault-bend fold style). Liassic marls favor minor décollement levels. Beneath the anticline, duplication of the Mesozoic cover is observed. In the study area, thrust-related folds are a mixture between the three types of fault-related folds described above.

DIXON & LIU (1992) have observed a similar evolution from centrifugal structural models; these represent a stratigraphic succession composed of six units with alternating bulk competency (low competence at the base). The models were subjected to horizontal, layer-parallel compression and show three mechanisms of shortening: layer-parallel shortening, buckling and thrust faulting. The relationship between folding and faulting evolves through time: firstly, detachment buckle folds form above a zone of décollement, secondly, a fault ramp propagates upward across the lowermost competent layers at the position of a foreland dipping limb (fault-propagation fold) and thirdly, when the fault has propagated through the competent unit its trajectory bends into the overlying incompetent unit and with further transport the hangingwall is modified by fault-bend folding. Limbs of the low-amplitude folds form shortly afterward, cut by foreland verging thrust faults.

The question, about the core infill of Jura anticlines, has been debated by geologists since the beginning of the century (BUXTORF, 1907). Using the same dip data, based on surface geology, several type of cross-sections have been drawn. As discussed by BITTERLI (1992), the core of an anticline may be filled by salt flow, duplexes, duplication of the entire cover over a thrust or thrust sheets presenting several generations of thrusting. In the absence of seismic data, several different methodologies have been tested in the Jura foreland fold and thrust belt, by different geologists, in order to answer this question: analogical modeling, comparison with other foreland belts, 2D and 3D modeling and new models of folding (BITTERLI, 1988; PHILIPPE, 1995).

In the central Jura (this work), the wealth of seismic data has allowed clarification of the geometry beneath the anticlines. The Haute Chaîne folds are first related to evaporite stacks within the Triassic layers and then evolved over thrust faults, which implies duplication of the Jurassic cover. In the Plateau Jura, the cores of the broad folds (not related to thrust) are filled with evaporite stacks.

For the southern French Jura, the recent PhD thesis of PHILIPPE (1995) interprets the evolution of folds as asymmetric detachment folds with salt flow that later evolve into fault-propagation folds. This is compared herein with analog modeling and with examples from the Canadian Rocky Mountain Foothills and Front Ranges described by DOBSON & MCCLAY (1992) and LANGENBERG (1992). Folds are first related to evaporite flow and then to thrust faults that duplicate the strata.

In the eastern Jura, cross-sections were constructed for many years in the style of lift-off folds (box folds), supported by thickening of lower Jurassic to Triassic sediments in their core, as drawn already by BUXTORF (1916) at the beginning of the century (see Figure 1.5, Section 2). However, modeling in two (balanced cross-sections) and three dimensions (block mosaic) of the geometry and the kinematics of one of these eastern anticlines (Weissenstein), has lead to a completely different interpretation (BITTERLI, 1990). The huge lift-off box folds are reinterpreted in terms of complex fault-bend folds presenting at least two generations of thrusting. However, these large thrusts are nowhere exposed at the surface.

LAUBSCHER (1986, 1992), using seismic evidence, has suggested that some of the eastern Jura box folds e.g. the Grenchenberg (Fig. 1.5) are supported by hinterland-dipping stacks, within the Middle Triassic Anhydritgruppe (= Triassic Unit 2) duplexes. Thrusts may be hidden in the subsurface.

In the eastern Jura also, JORDAN & NOACK (1992) have discussed the geometry of thrusts related to thick ductile soles. The model they propose differs from the classical fault-bend fold model, which has only a discrete sole thrust fault. The backlimb is much longer than the present ramp and has a lower backlimb angle with respect to the ramp angle. Several differences concerning rotation and migra-

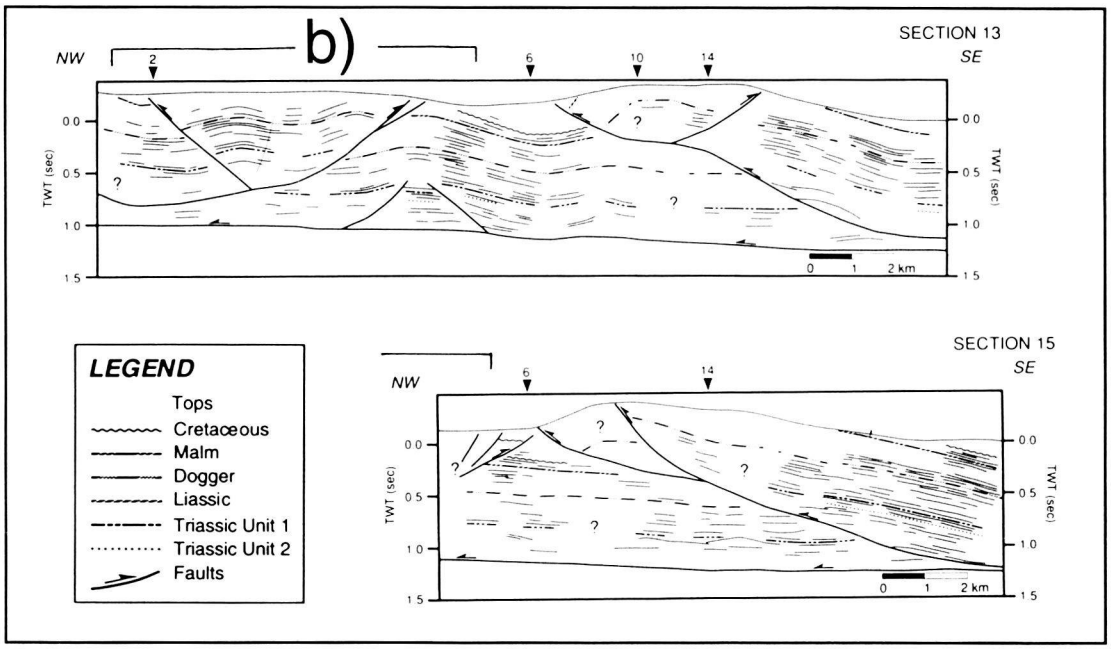

a)

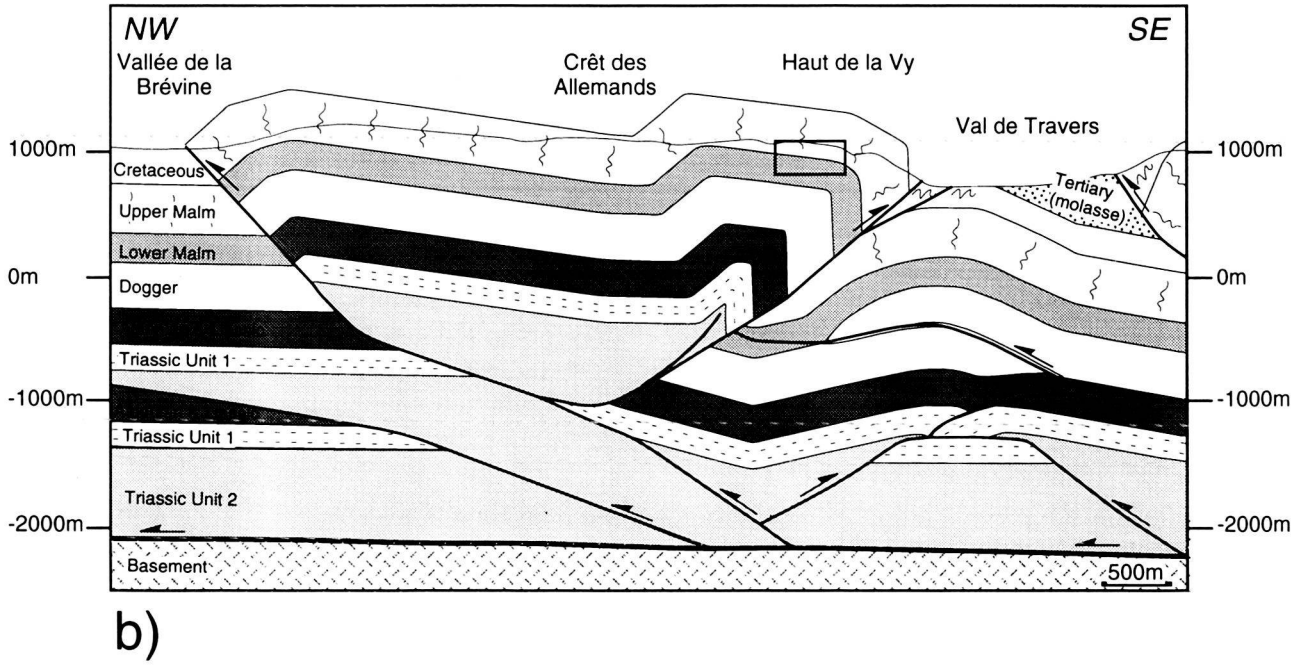

b)

Figure 3.17 (pages 100, 101): Deformation at different scales in a hinterland-vergent anticline from the Neuchâtel Jura (Val de Travers area). Figures 3.17c and d are according to PFIFFNER (1990).

a) Line drawing (in TWT depth scale) of seismic Section 13 and 15 illustrating the regional scale.

b) Geological cross-section according to seismic interpretation and outcrop data. The rectangle shows the location of the small scale folds illustrated in Figure 3.17c. For location of the cross-section, see Figures 4.7b and 4.9.

c) Detailed cross-section showing relationships between meter scale folds and faults. Rectangle locates Figure 3.17d.

d) Detailed analysis (meter scale) of one of the small scale folds of Figure 3.17c.

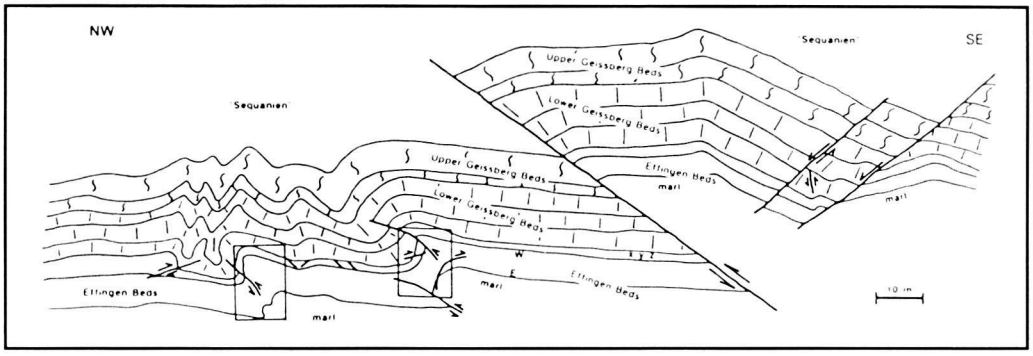

c)

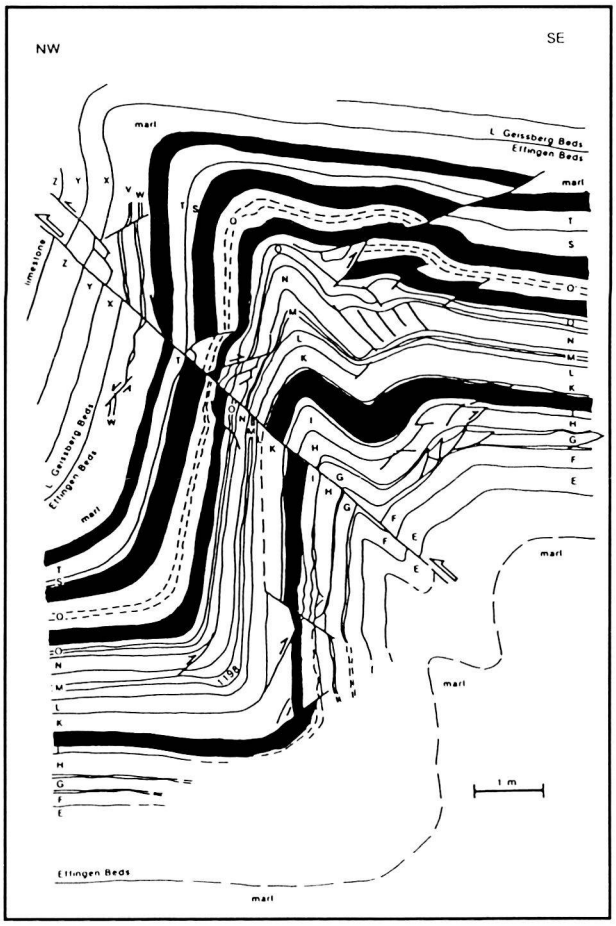

d)

Déformation à différentes échelles au sein d'un anticlinal à vergence vers le SE localisé dans le Jura neuchâtelois (Val de Travers). Figures 3.17c et d sont modifiées de PFIFFNER *(1990).*

a) Réflecteurs (profondeur en temps) des profils sismiques 13 et 15 (échelle régionale).

b) Coupe géologique en accord avec l'interprétation sismique et les données de la géologie de surface. Le rectangle montre l'emplacement des plis décamétriques illustrés dans la Figure 3.17c. Localisation de la coupe, voir Figures 4.7b et 4.9.

c) Coupe géologique détaillée montrant les relations entre les plis décamétriques et les failles. Le rectangle localise la Figure 3.17d.

d) Analyse détaillée d'un pli métrique de la Figure 3.17c.

tion of hinges are presented. In this model, a major part of the backlimb is deformed only by layer parallel slip, because it does not migrate through the flat-ramp hinge. These authors present some field evidence (a more or less intact backlimb), which seems to confirm the last point. This model also presents some features compatible with the central Jura, notably a thick ductile sole thrust and long shallow dipping backlimbs e.g. Chaumont anticline (Fig. 4.5).

In conclusion, the Haute Chaîne Jura folds of the central Jura developed first as buckle folds (detachment folds) and then evolved into fault-propagation or/and fault-bend fold types. The presence of a thick and very weak sole thrust and the final geometry of the folds has led to this model. The first stage buckle folds were most probably similar to the Plateau Jura evaporite-related folds. Seismic profiles are a good tool for understanding the geometry of the folds, but 3D kinematic modeling would allow to further constrain the geometry and also include the lateral continuation of the anticlines.

3.3. TEAR FAULTS

3.3.1. Definitions

In the following paragraphs, the general context of strike-slip faults is discussed first, followed by more specific discussion and definition of tear faults.

a) Strike-slip faults (sensu lato)

Strike-slip faults correspond to the end member of the spectrum in a kinematic classification of faults (REID *et al.*, 1913). According to the definition of BATES & JACKSON (1987), they represent "faults on which most of the movement is parallel to the faults' strike". They are generally vertical and accommodate horizontal shear within the crust or/and the lithosphere. Displacement along these faults may be either right-lateral or left-lateral. SYLVESTER (1988), reviewing strike-slip faults (Fig. 3.18), suggested that such faults can be classified either as transform faults, which cut the lithosphere as plate boundaries, or as transcurrent faults which are confined to the crust. The latter category, which includes indent-linked strike-slip faults, tear faults, transfer faults and intracontinental transform faults, is of particular interest in the study of thin-skinned fold belts, such as the Jura.

Indent-linked strike-slip faults juxtapose pieces of continental lithosphere, especially in zones of plate convergence and tectonic escape. They are not true transform faults, because they do not cut the lithosphere. Tear faults accommodate the differential displacement within a given allochthon or between the allochthon and adjacent structural units. They are generally oriented transverse to the strike of the deformed rocks and are sometimes called transverse faults or transcurrent faults. The term transfer fault is used for strike-slip faults that connect overstepping segments of parallel or en echelon strike-slip faults. Commonly located at the ends of pull-aparts, they transfer the displacement across a stepover from one parallel fault segment to the other. Intraplate or intracontinental transform faults are regional strike-slip faults, which are similar to indent-linked strike-slip faults in that they are restricted to the crust, but they need not to be genetically related to indentor tectonics. They typically separate regional domains of extension, shortening or shear.

Transfer faults and intracontinental transform faults are of larger scale than tear faults and also may accommodate larger amounts of slip (TWISS & MOORES, 1992). Tear fault seems to be the appropriate term to characterize the strike-slip faults observed in the Jura.

b) Tear faults

To our knowledge, there is no generally admitted, precise definition of tear fault. In this paragraph, definitions proposed by different authors are presented to avoid confusion with this term.

DAHLSTROM (1970) probably published one of the first definitions and classifications of tear faults: "a tear fault is a species of strike-slip fault which terminates both upwards and downwards against movement planes, that may be detachments or thrust faults or low angle normal faults". He distinguishes two basic types of tear faults: 1) transverse (primary or secondary) or oblique tear fault within a deformed thrust sheet; 2) tear fault as an integral part of a thrust sheet boundary. The first type is discussed below; for the second, one may refer to Dahlstrom's explanations.

In primary tear faults, the amount of shortening on either side is consistent, but the mechanisms may be different. Such compensated differences in rock shortening mechanisms demonstrate that the tear fault is an integral part of the structural fabric, which developed in the very early stages of deformation.

Secondary transverse tear faults provide a mechanism for transferring displacement between pairs of existent thrust faults. Such tear faults transect the intervening thrust sheet, thus permitting adjacent parts of the same thrust sheet to have markedly disparate displacements. Formation of these tear faults post-dates thrusting and they are therefore secondary phenomena.

According to the SYLVESTER's (1988) classification of strike-slip faults (Fig. 3.18), tear faults belong to the category of transcurrent faults found in intraplate settings (thin-skinned). For the exact definition of tear faults, Sylvester refers to BIDDLE & CHRISTIE-BLICK (1985): "a strike-slip fault or oblique-slip fault within or bounding an allochthon produced by either regional extension or regional shortening. Tear faults accommodate differential displacement within a given allochthon and adjacent structural units". In this classification, strike-slip fault as mentioned above, is not a specific term, but a generic term.

In structural geology books e.g. TWISS & MOORES (1992), the term tear fault is used in a general sense, describing as a small-scale, local strike-slip fault, that is commonly subsidiary to other structures such as folds, thrust faults, or normal faults. They are steeply dipping and oriented subparallel to the regional direction of displacement. They occur in the hangingwall blocks of low angle faults and accommodate different amounts of displacement, either on different parts of the fault or between the allochthon and adjacent autochthonous rocks. The discontinuity in displacement is then taken up by tear faults. Tear faults within a deformed sheet per-

CLASSIFICATION OF STRIKE-SLIP FAULTS

INTERPLATE (deep-seated)	INTRAPLATE (thin-skinned)
TRANSFORM faults (delimit plates, cut lithosphere, fully accommodate motion between plates)	**TRANSCURRENT faults** (confined to the crust)
Ridge transform faults* • Displace segments of oceanic crust having similar spreading vectors • Present examples: Owen, Romanche, and Charlie Gibbs fracture zones	Indent-linked strike-slip faults* • Separate continent-continent blocks which move with respect to one another because of plate convergence • Present examples: North Anatolian fault (Turkey); Karakorum, Altyn Tagh, and Kunlun fault (Tibet)
Boundary transform faults* • Join unlike plates which move parallel to the boundary between the plates • Present examples: San Andreas fault (California), Chaman fault (Pakistan), Alpine fault (New Zealand)	Tear faults • Accommodate differential displacement within a given allochthon, or between the allochthon and adjacent structural units (Biddle and Christie-Blick, 1985) • Present examples: northwest- and northeast-striking faults in Asiak fold-thrust belt (Canada)
Trench-linked strike-slip faults* • Accommodate horizontal component of oblique subduction; cut and may localize arc intrusions and volcanic rocks; located about 100 km inboard of trench • Present examples: Semanko fault (Burma), Atacama fault (Chile), Median Tectonic Line (Japan)	Transfer faults • Transfer horizontal slip from one segment of a major strike-slip fault to its overstepping or en echelon neighbor • Present examples: Lower Hope Valley and Upper Hurunui Valley faults between the Hope and Kakapo faults (New Zealand), Southern and Northern Diagonal faults (eastern Sinai)
	Intracontinental transform faults • Separate allochthons of different tectonic styles • Present example: Garlock fault (California)

*See Woodcock (1986, p. 20) for additional examples, both ancient and modern, and for their geometric and kinematic characteristics.

From Sylvester 1988

Figure 3.18: Classification of strike-slip faults from SYLVESTER (1988). See also WOODCOCK (1986).

Classification des décrochements (sensu lato) d'après SYLVESTER (1988). Voir aussi WOODCOCK (1986).

mit abrupt changes in the pattern of deformation through differential movement between component parts of the sheet. Displacement may be either right-lateral or left-lateral. Twiss & Moores define a strike-slip fault as a vertical fault that accommodates horizontal shear within the crust. Strike-slip faults exist on all scales, in both oceanic and continental crust.

In his glossary of thrust tectonic terms, McClay (1992) defines tear faults as strike-slip faults parallel to the thrust transport direction and separating two parts of the thrust sheet, each of which has a different displacement. He distinguishes a tear fault from a lateral ramp; the latter is a ramp in the thrust surface parallel to the direction of transport of the thrust sheet. Ramp angles are generally between 10° and 30°. He notes that if the lateral structure is vertical then it becomes a thrust transport parallel tear or strike-slip fault and should not therefore be termed a lateral ramp.

All these explanations or definitions highlight many geometric and kinematic peculiarities of tear faults admitted by most authors. In summary:

- *a tear fault belongs to an allochthonous sheet and has a transcurrent movement*
- *a tear fault terminates rightward and leftward into a thrust fault and downward into a décollement zone*
- *a tear fault is steeply dipping*:
  Lateral ramps like tear faults are subparallel to the transport direction. Tear faults have a subvertical fault plane, whereas lateral ramp fault planes dip 10° to 30° (Fig. 3.19).
- *the same amount of shortening may be accommodated differently on each side of the fault*
- *the formation of a tear fault may be earlier and contemporaneous to thrusting (primary tear fault) or subsequent (secondary tear fault)*:
  In primary tear faults, shortening may be accommodated differently on each side of the fault i.e. one thrust-related fold on one side may correspond to two thrust-related folds on the other side. In this case it is difficult to determine a sense of movement. Therefore on a geological map, the sense of movement of primary tear faults is only apparent and the true displacement will be deduced from restored maps or from fault/striae outcrops in the field. However, in the case of secondary tear faults, the sense of movement is real and fold axes are offset as passive markers.
- *the tear fault is oriented subparallel to the regional transport direction of displacement*:
  A regional transport direction is difficult to determine in fold and thrust belts, where no direct access to the basal thrust planes exists. Intuitively, transport direction is perpendicular to fold axes. But in many cases, local transport direction is oblique to the regional direction. Therefore it would be more appropriate to define the trend of the tear faults in comparison with the fold belt orientation.

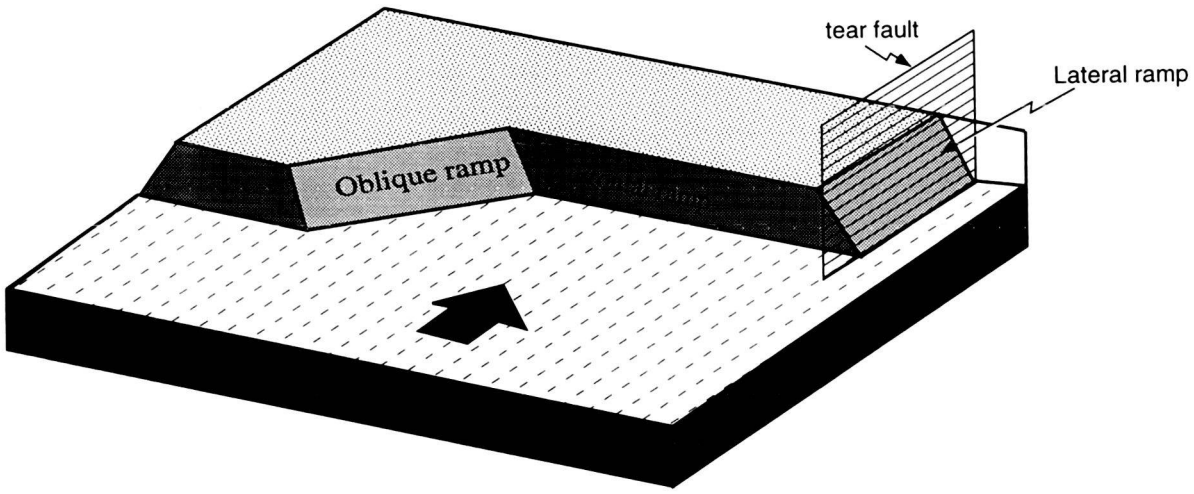

Figure 3.19: Three-dimensional view of a tear fault and different ramp types (lateral, frontal and oblique ramps).

Vue tridimensionelle d'un décrochement (sensu stricto) et de différentes rampes (rampes latérale, frontale et oblique).

Ramps are often associated with tear faults. There are basically three types of ramps: frontal, oblique and lateral (Fig. 3.19). These ramps are defined with respect to the regional transport direction, perpendicular, oblique and parallel respectively (APOTRIA *et al.*, 1992). Fault planes of these ramps generally show dips between 10° to 30°.

3.3.2. Geomorphological evidence

The tear faults in the Jura are well known from geological maps but can almost as well be recognized on topographic maps, where they have a clear morphological expression (Fig. 3.20). A close genetic relationship between folding and tear faults was postulated by HEIM (1915), who noted the radial arrangement of the tear faults when viewed on a map of the entire Jura arc. Major, apparently sinistral, tear faults are oriented NW-SE in the southern Jura, NNW-SSE to N-S in the central Jura and NNE-SSW in the eastern Jura (Fig. 3.20a). Somewhat shorter, apparently conjugate dextral tear faults are often associated. Folds, thrusts, sinistral and dextral tear faults define a set of structures compatible with a horizontal shortening in a WNW-ESE, NW-SE, and NNW-SSE direction respectively (LAUBSCHER, 1972, indenter model).

On the geomorphological map (Fig. 3.20b), tear fault traces appear to be straight lines even across rugged topography. Tear faults are marked by prominent continuous topographic features, such as narrow linear depressions. The topographically high part of the fault changes from one side to the other along the fault trace, because of the juxtaposition of different structures along the fault (synclines and anticlines) e.g. Pontarlier fault, or the juxtaposition of lithologies with different resistance to erosion. It is important to highlight this morphologic evidence, because as will be discussed below, seismic characterization of tear faults may be poor in some cases (e.g. La Ferrière fault, La Tourne fault).

In addition, geological maps present also evidence for tear faults; fold axes tend to terminate against tear faults and they do not have obvious direct correlation from one side of the fault to the other (see later discussion).

3.3.3. Geophysical evidence from seismic profiles

Generally, geophysical evidence for an important tear fault includes a transparent zone without reflections, a different succession of stratigraphic reflectors on either side of the fault and an offset of the corresponding seismic reflectors from one side to the other. The transparent zone may be wide or narrow (<1 km). On the studied lines, large transparent zones without reflectors are recognized in Panel 7 and Panel 8.

In this respect, seismic lines and cross-sections, are not ideal for the analysis of strike slip tectonics. Strike-slip faults are best analyzed on the horizontal plane of geological or geomorphological maps, which are natural sections at a high angle and contain the dominant displacement vector. Strike-slip faults may produce a series of characteristic features on seismic sections such as the well known positive and negative flower structures. Positive identification of such structures is not easy, however, and would ideally require a three-dimensional survey or at least a series of lines across the same fault zone.

3.3.4. Examples illustrated by seismic profiles

Some seismic lines cross major mappable Jura tear fault zones, e.g., the Morez (France), Mouthe (France), Pontarlier (France-Switzerland), Mt Chamblon-Treycovagnes (Canton Vaud), La Tourne and La Ferrière-Vue des Alpes (Canton Neuchâtel) zones (Fig. 3.19; Panel 3, 5, 6, 7 and 8). On seismic lines, it can be seen that these faults affect the whole Cenozoic and Mesozoic layers of the Jura and Molasse Basin cover.

In the Canton Vaud, seismic data, crossing the southern part of the major Pontarlier tear fault, are of high quality on both sides of the fault (Panel 7). Section 46 (Panel 7) displays a succession of well layered reflectors, whose stratigraphic interpretation is well constrained laterally. From one side to the other, stratigraphic thickness changes are observable within the Dogger - Liassic beds and within the Triassic Unit 2 layer. The latter is thicker on the western side of the fault, which may explain the higher elevation for the same beds on the western side of the fault. Section 50 (Panel 7) presents also a succession of layered reflectors on both sides of the tear fault. They are unfortunately not well constrained by other seismic lines (Figs. 1.4 and 4.1). The attempted interpretation shows a thickening of the Malm and the Triassic Unit 2 layers on the western side of the fault.

Further north, in the Lake Joux area (Panel 8), the quality of seismic data along the Pontarlier tear fault

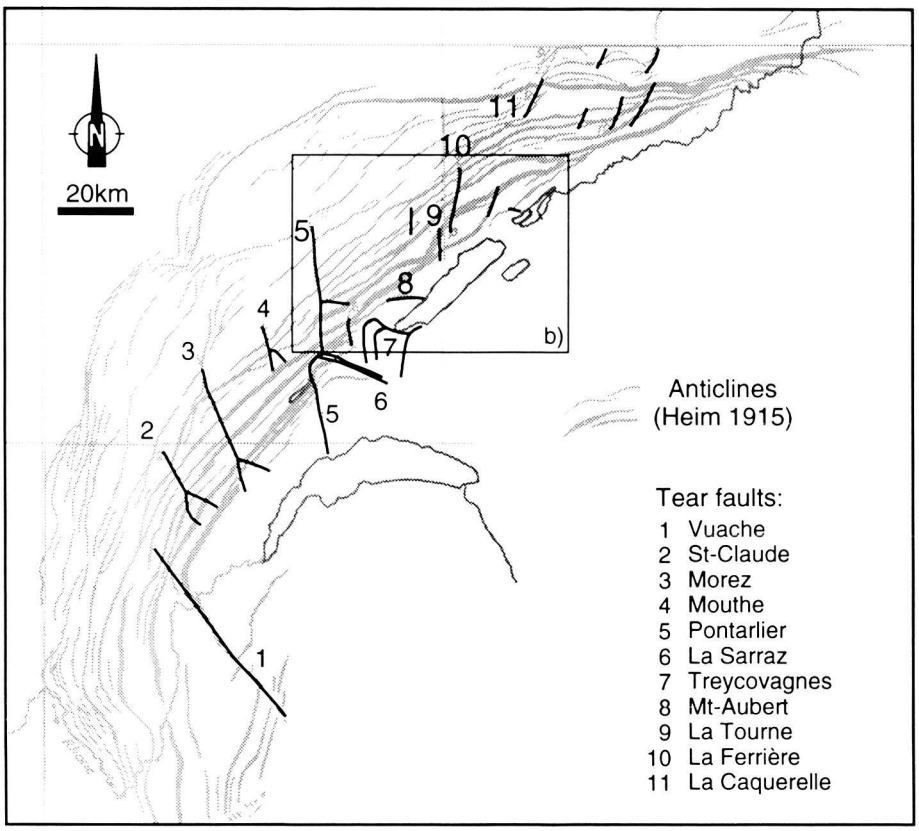

a)

b)

Figure 3.20:
a) Location of tear faults on Jura anticline map drawn by Heim (1915).

b) Geomorphological evidence of tear faults in the central Jura.

a) Situation géographique des décrochements sur une carte des axes des anticlinaux de Heim (1915) de la chaîne du Jura.

b) Evidence géomorphologique de décrochements dans le Jura central.

is poor. Unfortunately the seismic lines end close to the fault. In this case, no stratigraphic correlation is possible on the western side of the fault. The Sarraz tear fault forms the conjugate dextral system to the sinistral Pontarlier fault and is displayed on Section 26 (intersection 36, Panel 4) and on Section 36 (intersection 26, Panel 6). Along the Pontarlier tear fault, seismic data do not give evidence for basement offsets. The tear fault appears to terminate in the décollement level of Triassic Unit 2.

The Yverdon area (Figs. 1.2, 1.4 and 4.3) is another region with conjugate tear faults (JORDI, 1993). Recently, a careful structural investigation (CHYN, 1995) for hydrogeological purposes has led to a detailed interpretation of seismic lines in this region (Section 27 on Panel 5; Section 38 on Panel 6). The regional setting and results will be discussed in Chapter 4. These faults appear to be tear faults and thrust faults. The associated structure is a fold related to a northward-vergent thrust, cutting the frontal fold limb (Fig. 4.18). Thickness changes within the Dogger beds are observable, showing a thickening towards the South. This local change (not clearly visible on the regional isopach maps of the western Molasse Basin, Fig. 2.26) may be due to lateral facies changes.

In the Neuchâtel area, seismic data along tear fault zones of La Tourne (Section 7 on Panel 1 and Section 4 on Panel 3) and La Ferrière-Vue des Alpes (Section 3, Panel 1) are of poor quality, probably due to the presence of an anticline on one side of the faults. These faults appear on seismic lines as transparent zones. No offset of the basement top on either side of the fault could be detected from contour maps. Accordingly, these faults are either tear faults restricted to the cover or lateral ramps. No evidence for an extension of these faults into the basement could be found.

3.3.5. Description from outcrops

Four major, N-S oriented tear faults are found within the study area (Fig. 3.20): Pontarlier, La Tourne, La Ferrière and Treycovagnes. All these faults have apparent sinistral offsets of a few hundred meters and their traces can be followed over several kilometers. Conjugate dextral faults e.g. La Sarraz, Mt-Aubert oriented 120° are associated with them.

In addition to these large, map scale tear faults, an important number of minor faults are observed in the competent lithologies of the central Jura e.g. (LLYOD, 1964). These minor faults have a less important throw (on the meter scale) and crosscut anticlines, but they are often too small to appear on geological maps. The poor outcrop quality, in many parts of the Jura, usually prohibits the direct observation of the effect of such minor structures on geological limits.

In the Val de Ruz (Neuchâtel Canton), small scale (cm to dm offsets) striated faults are ubiquitous in limestones and most outcrops show a sufficient number (>20) of fault/slickenside pairs for statistical determination of "paleo-stress" or strain axes directions. TSCHANZ & SOMMARUGA (1993) conducted a kinematic analysis of fault/slickenside pairs using ANGELIER & MECHELER's (1977) right dihedra method. Similar observations have been made in other parts of the Jura and have led different authors (DROXLER & SCHAER, 1979; LAUBSCHER, 1979; PFIFFNER, 1990; TSCHANZ, 1990) to independently draw a comparable schematic diagram of the relation between faults and folds (Fig. 3.21). Strike-slip and thrust faulting occurs during the early stages of folding and is interpreted as due to large parallel shortening preceding folding. During fold amplification, these earlier faults are passively rotated with the fold limbs and partly reactivated to accommodate internal deformation related to folding.

Fault/slickenslide analyses from the vicinity of large strike-slip movement zones indicate systematically subhorizontal movement directions, despite variable bedding orientations. Horizontal striations on vertical fold limbs are frequently observed (e.g. La Tourne or La Ferrière-Vue des Alpes) and clearly indicate that some fault motion post-dates folding. Local maximum compression axes, determined from fault/slickenside pairs and twin strain analyses, are systematically oriented subperpendicular to the local fold axis trend, but major discrepancies exist between this general NW-SE compression direction and the map scale fold axis trends.

Fault/slickenside analyses preferentially measure late (with respect to folding) strain increments, due to the sampling of fault planes, because late, subvertical tear faults are much easier to detect in the field than supposedly earlier, layer-parallel fault planes. The predominance of subhorizontal shortening and extension directions as determined from fault/slickenside pairs is partly due to this sampling effect. Nevertheless, the results show that NNW to NW directed shortening was active throughout the fol-

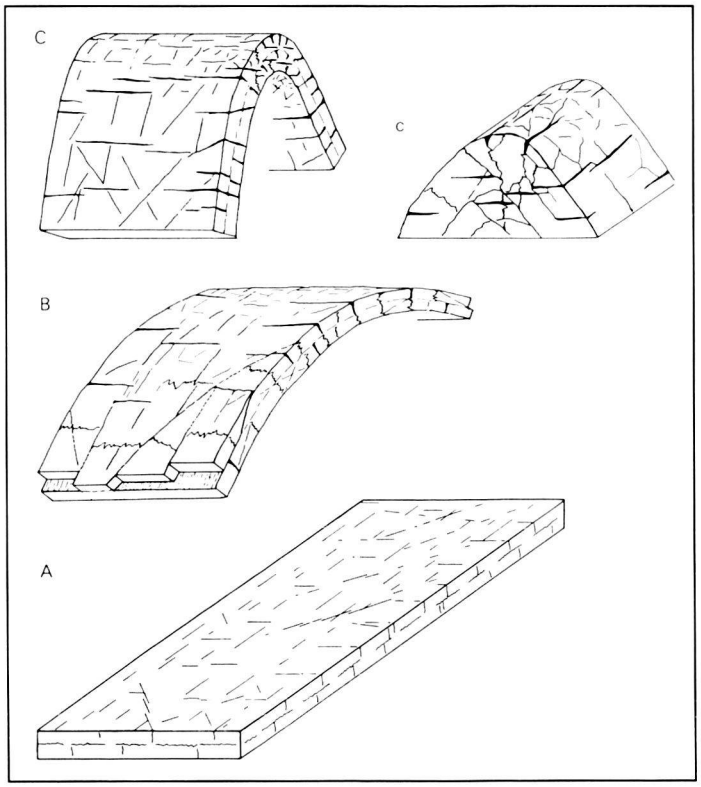

From Droxler & Schaer 1979

Figure 3.21: Relation between faults and folds during amplification of a metric fold in limestone rocks. A) Layer parallel shortening before folding; B) Fold amplification, 30% shortening; C) 60% or more shortening. From DROXLER & SCHAER (1979).

Relations géométriques entre faille et pli durant la mise en place d'un pli métrique dans des roches calcaires. A) Avant le plissement, lorsque le raccourcissement est parallèle aux couches; B) Durant l'évolution du pli, lorsque 30% de raccourcissement est observé; C) à 60% ou plus de raccourcissement. Tiré de DROXLER & SCHAER (1979).

ding history. This shortening seems to be still active today, as evidenced by in situ stress determinations (BECKER, 1987; BECKER, 1989; SCHAER *et al.*, 1990; BECKER & WERNER, 1995) and focal mechanisms from earthquakes (PAVONI, 1984; DEICHMANN, 1992). According to Deichmann, the focal mechanisms are of strike-slip or normal fault type, indicating a regional shortening with a NNW-SSE orientation, roughly perpendicular to the strike of the Alpine and Jura belt and a corresponding WSW-ENE extension parallel to the main axis of the Molasse Basin. Hypocenters below northern Switzerland are distributed throughout the entire depth range of the crust. This distribution of focal depths contrasts with what is observed below the Alps and in most other intracontinental settings.

3.3.6. Interpretation of the central Jura and Molasse Basin tear faults

Major tear faults (from West to East: Vuache, Morez, Pontarlier and La Ferrière, Fig. 3.20) cut the Jura belt at angles of 60°-70° to the fold axes. Many minor faults are associated to the major ones. All these faults have an apparent sinistral movement and change from a NW-SE to N-S trend along the Jura arc. Conjugate dextral sets of tear faults are less developed, nevertheless, the Sarraz and the Treycovagnes faults are good examples. The major tear faults are located in the Haute Chaîne Jura and are connected to thrust planes at the transition Haute Chaîne - Plateau Jura. On seismic lines these faults represent important transparent zones, indicating that these faults are characterized by broad deformation zones.

Folds tend to terminate against tear faults and do not match from on side of the fault to the other (e.g. Pontarlier fault, Fig. 3.22). AUBERT (1959), LAUBSCHER (1965), PHILIPPE (1995) and SCHÖNBORN (1995) have attempted correlation from one side of Pontarlier fault to the other. Each author has proposed a different correlation, requiring lengthy arguments to justify a far from obvious choice. Most probably, there is no match to be found because shortening was accommodated by different fold trains on either side of the fault. These observations lead to the interpretation of the Pontarlier fault as a primary tear fault, i.e. differential movements along this fault occurred during folding (DAHLSTROM, 1970). Fault/slickenside outcrop observations on tear faults cutting anticlines show that striae dip is rarely bedding parallel on the vertical limb, but is mostly horizontal. The latter observation favors post-folding movement along the fault. Although offsets of geological limits appear to be mostly

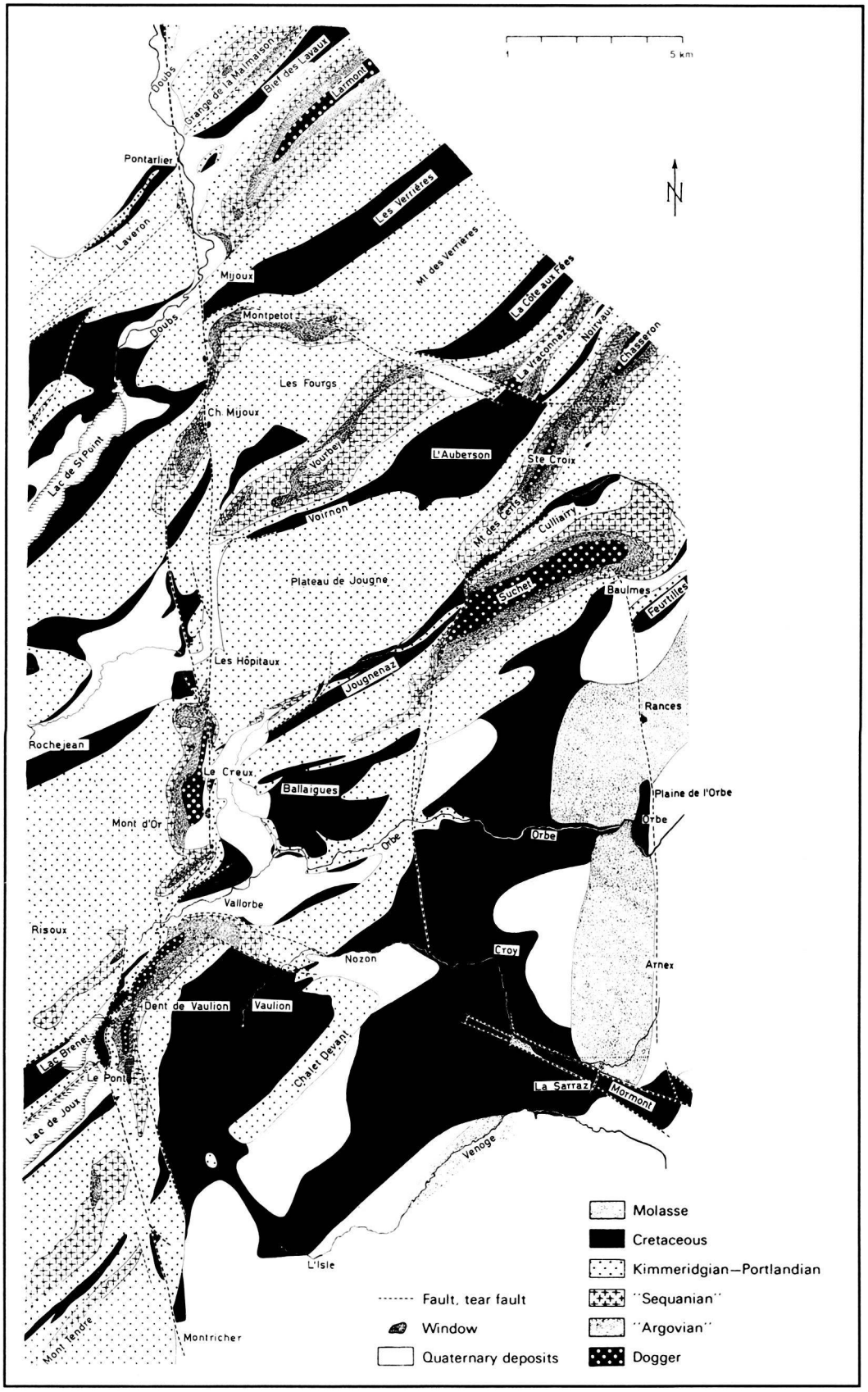

From Aubert 1959

Figure 3.22: Simplified geological map along the Pontarlier tear fault (see for location Figures 1.2 and 3.20). From AUBERT (1959).

Carte géologique simplifiée le long du décrochement de Pontarlier (pour localisation voir Figures 1.2 et 3.20). Tiré de AUBERT (1959).

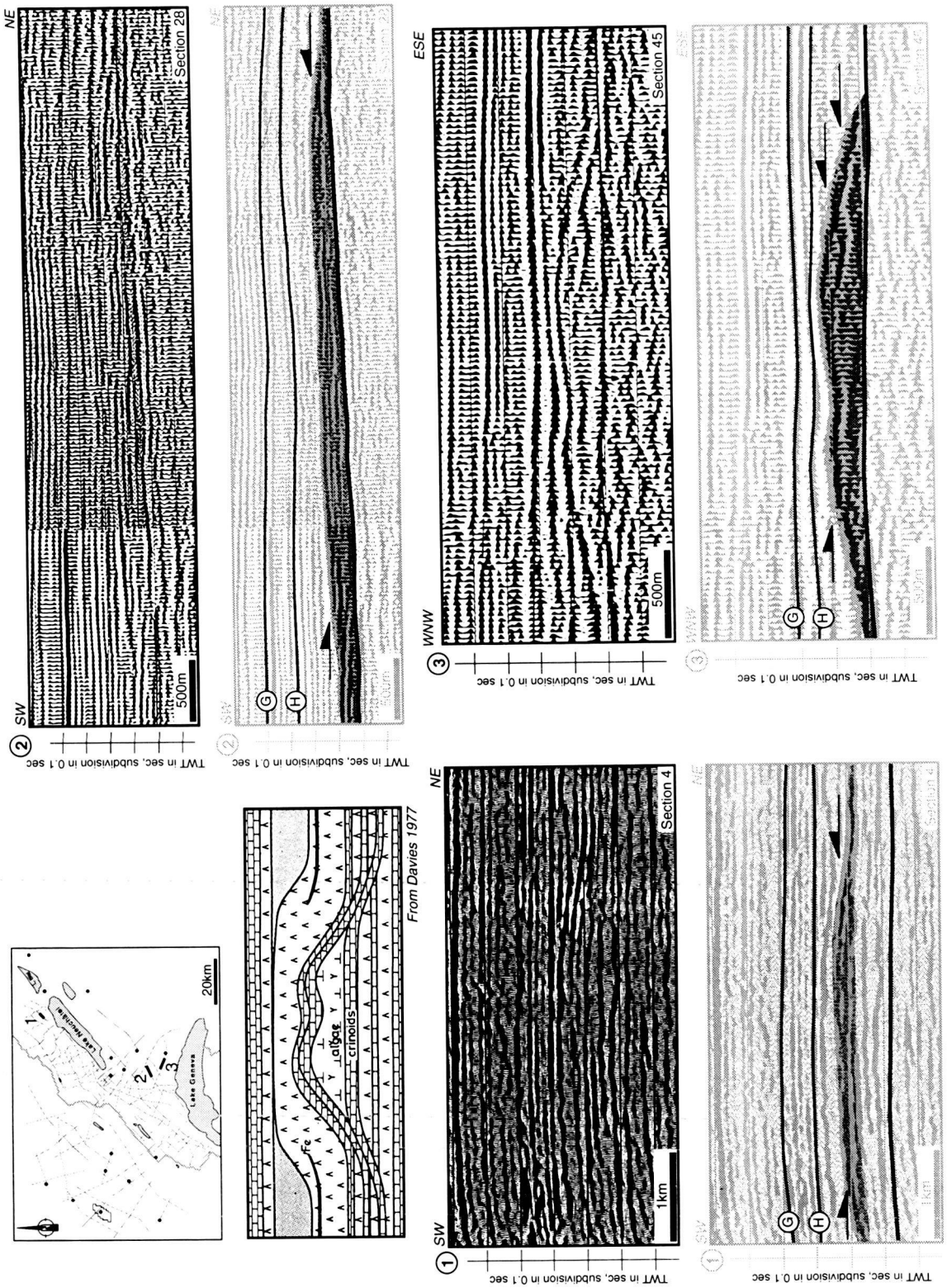

Figure 3.23: Portions of seismic lines showing oblique reflectors in the Triassic Unit 2 interval, which is not thickened. These features do not affect the overlying strata by buckling and could be interpreted as reef-like features in comparison with the algal mound developed in carbonate-anhydrite facies in the Canadian Arctic Archipelago (DAVIES, 1977) or as dissolution effects (see text for discussion). Legend for the top of the layers: G = Triassic Unit 1, H = Triassic Unit 2.

Portions de profils sismiques montrant des réflecteurs obliques dans l'intervalle de l'Unité 2 du Trias, qui n'est pas épaissie. Ces particularités dans le Trias n'affectent pas les couches sus-jacentes en les plissant. Elles peuvent être interprétées soit comme des structures récifales, en les comparant aux accumulations algaires développées dans les faciès évaporitiques carbonatés de l'Archipel arctique canadien (DAVIES, 1977), soit comme le résultat d'effets de dissolution (voir texte pour discussion). Légende pour le toit des couches: G = Unité 1 du Trias; H = Unité 2 du Trias.

sinistral on the map scale, there is no objective way to determine absolute displacements along this tear fault, because folding occurred at least partly syn-faulting. It is therefore concluded, that the Jura tear faults show mainly syn-folding and post-folding movement.

In this study, no evidence for deeply rooted strike-slip faults has been observed on the seismic sections. Faults root in the main ductile zone (Triassic Unit 2) and apparently do not offset the underlying basement. HEIM (1921, p.614) already suggested that tear faults rooted in the cover only. Consequently, these faults have been correctly named as tear faults, because they belong to an allochthonous sheet.

3.4. "REEF-LIKE" FEATURES

As explained in preceding paragraphs, the Triassic Unit 2 interval varies in thickness and often presents oblique reflectors on the seismic lines. Some of these features have been interpreted as tectonic structures (duplexes, see Figure 3.8 and Fig. 3.12) just above the main décollement horizon. They show a thickening within the Triassic Unit 2, with folds in the overlying beds. However, other examples that also show oblique reflectors in the Triassic Unit 2 layer, are not associated with thickening in the Triassic beds or buckling of the overlying strata (Fig. 3.23); accordingly, they seem to be formed during Triassic times. The nature of these features is the subject of this section.

These features resemble biogenic reef structures or algal mounds like those of Mississippian-Pennsylvanian age, found in carbonate-anhydrite facies from the Canadian Arctic Archipelago (DAVIES, 1977) (Fig. 3.23). The Zechstein salt facies also show this type of feature. JENYON & TAYLOR (1987) and TAYLOR (1993) discuss the possible confusion of such features with buildups and propose the terms "reef-like features" or "pseudo-reefs", respectively. According to Jenyon & Taylor, some of these positive features resting on basal Zechstein, consist of material of much higher velocity than salt and may be bryozoan-algal reefs from their shape and location. However, it is equally possible that they may be primary or relict pods of anhydrite resulting from dissolution and removal of the surrounding salt. For Taylor, the mound-like features are related to swelling in Zechstein evaporite intervals. Virtually all are situated below former pillows in the overlying salt and many are related to faults. Careful seismic interpretation in the Zechstein basin reveals that the reflector defining the top of these structures is broken into segments, each of which is offset. In many cases, there is no velocity anomaly beneath these pods. Therefore the included material should have more or less the same velocity as the adjacent rocks. Pure salt (~ 4500 m/s) does not have the same velocity as carbonates (~5500 m/s to more than 6000 m/s), whereas anhydrites may be in the same range of velocity as carbonates.

Algal mounds within the German Triassic facies are not known from field observations (A. Baud at the Musée de Géologie in Lausanne, oral communication). However, only very few Triassic beds crop out in the Jura Mountains and none in the Molasse Basin. Even in areas where Triassic strata crop out, such as around the rim of the Vosges and Black Forest, evaporite (NaCl)-bearing series are exceedingly rare at outcrop and always strongly perturbed by surface weathering. In the absence of high resolution seismic lines and with the sparse drill hole information available, it is impossible to discard any of these hypotheses. This issue is not without bearing on the hydrocarbon potential of the area: carbonate buildups within evaporite series, if present, may be interesting traps.